ABSTRACT

CHEN, YUFEI. Selective Drug Screening Method Development using Nanofibers and Microfluidics Coupled to a Quadrupole Time-of-Flight Mass Spectrometry. (Under the direction of Dr. Nelson Vinueza Benitez).

Drug analysis plays an important role in the forensics field, especially nowadays were an opioid crisis is on the rise worldwide. An ideal on-site drug analysis system should provide reliable qualitative and quantitative results with minimal sample preparation. Recently, a new microfluidic device (MFD) developed at NC State University, used for the extraction of dyes from trace fibers was used tested for drug analysis and its capabilities were further explored. The analysis and characterization of the drugs were performed on a quadrupole–time-of-flight (Q-TOF) mass spectrometer. The combination of electrospun nanofibers, microfluidics, and mass spectrometry provided a robust system for qualitative and quantitative analysis of drugs of forensic interest.

Selective Drug Screening Method Development using Nanofibers and Microfluidics
Coupled to a Quadrupole Time-of-Flight Mass Spectrometry

by
Yufei Chen

A dissertation submitted to the Graduate Faculty of
North Carolina State University
in partial fulfillment of the
requirements for the degree of
Doctor of Philosophy

Fiber and Polymer Science

Raleigh, North Carolina

2018

APPROVED BY:

Nelson Vinueza Benitez Chair of Advisory Committee	David Muddiman
Denis Fourches	Stephen Michielsen

BIOGRAPHY

Yufei Chen was born in Zhengzhou, Henan Province, China on March 13, 1989. He won the first prize of the Chinese Chemistry Olympiad (Henan Province Division) in 2006 and was admitted by Zhejiang University, which boasts one of the top three chemistry departments in China. At Zhejiang University Yufei received his Bachelor of Engineering in Polymer Materials and Engineering in 2011. During his senior year of undergraduate studies, Yufei began to work on the synthesis of hyper-branched aggregation induced emission polymers. He obtained a Master of Science degree in Textile Chemistry at NC State in 2015, where his research is currently focused on dyes, biofuels, and mass spectrometry.

ACKNOWLEDGMENTS

Here I express my sincere gratitude to my advisor, Dr. Nelson R Vinueza, for his visionary guidance, insightful advice and genuine supports in my Ph.D. program, without which this thesis would not have been accomplished to its least content. I would also like to thank our group member, Cody Zane, Emily Lichtenberger, Kelsey Boes, Nadia Sultana and Xinyi Sui, all of whom have been always so supportive, helpful and collaborative to the research work described here. In addition, I really appreciate the kindness, care and helpful experience offered by COT officers Traci Figura and Amanda Padbury. Finally, I would like to thank my parents and wife for their consistent support for my studies at NC State, and all those lovely close friends that I have made here in Raleigh. Thanks for all their generous supports whenever and wherever I needed. I feel so blessed to meet all of them in my exploration in the United States.

TABLE OF CONTENTS

LIST OF TABLES

LIST OF FIGURES

1. Introduction

Drug analysis plays an important role in forensics and pharmaceuticals areas. An ideal on-site drug analysis system should provide reliable qualitative and quantitative results with minimal sample preparation. Therefore, a multidimensional system for the drug analysis is needed to assist in the fast screening and identification. Mass spectrometry in combination with microfluidics and liquid chromatography can be a unique analytical tool for both purposes.

Electrospinning is a relatively new technique to produce continuous fibers with diameters down to a few nanometers. It has gained popularity in various fields such as medical materials, special textiles, filtration techniques, and nano-electronics.[1,2] The high surface-to-volume ratio makes nanofiber an outstanding material to be combined with microfluidics.

Recently, a new microfluidic device (MFD) was developed by Drs. Dow, Hinks, and Vinueza from NC State University, for the extraction of dyes from fibers. Current work expanded the application of this MFD to more areas such as drug analysis

The following literature review will discuss the importance and current challenges of drug analysis, the outstanding performance of electrospun nanofibers and the history and principles of mass spectrometry, as well as the coupled sample preparation technique of microfluidics.

1.1 Drugs Abuse and Drug Analysis

Accurate and rapid analytical systems are needed for drug analysis in the forensic and pharmaceutical fields. Drug abuse is a serious health risk to people no matter their ages and societies. Nowadays, this global problem is growing even faster with the appearance of new synthetic drugs.[3] In forensic chemistry analysis, drugs could be classified based on their pharmacological effect, where the most common are depressants, such as barbiturates and benzodiazepines; stimulants, such as amphetamines and cocaine; analgesics, such as opioids and psychotomimetics such as marijuana.a[4]

Currently, many commercial drug screening devices are based on immunoassay technologies.[5-7] These methods are rapid but just for presumptive testing of illicit drugs. In addition, mass spectrometry methods coupled with separation techniques such as Gas-chromatography(GC)-MS and HPLC-MS have been utilized[8] to provide confirmatory drug analysis. GC analysis is a common technique used in forensic labs because of the well-developed database. But since numerous modifications of listed drugs have been developed to circumvent legislative controls for their use, the lack of database is becoming a new challenge for drug characterization. Recently, HPLC became an ideal technique for analytes that do not volatilize easily such as thermally unstable compounds (e.g., LSD) and explosives. This means HPLC doesn't require derivatization of analytes. The ability to combine solvents, which can include buffers and aqueous solutions, can aid the analysis of different matrices like blood and urine. HPLC is commonly used in combination with UV-Vis detectors and MS. But both GC and LC require long time consumption for sample preparation and sample run.

An ideal on-site drug analysis system should provide reliable qualitative and quantitative results with minimal sample preparation. Therefore, a multidimensional system for the drug analysis is needed to assist in the fast screening and identification. Mass spectrometry with high resolution, offers great sensitivity and versatility, which in combination with microfluidics and liquid chromatography can be a unique analytical tool for both purposes.

1.2 Forensic science

Forensic science is the application of science to criminal and civil laws during the investigation, governed by legal standards of admissible evidence and criminal procedure. Crime Scene Investigation Procedure contains collection, preservation, and analysis of physical evidence. The careers practicing Forensic Science have been classified by the 11 sections of the American Academy of Forensic Sciences (AAFS): Criminalistics, Digital and Multimedia Sciences, Engineering Sciences, General, Jurisprudence, Odontology, Pathology and Biology, Physical Anthropology, Psychiatry and Behavioral Sciences, Questioned Documents and Toxicology.

1.3 Challenge of Forensic science

Forensic science is not as robust as society thought. In 2004 Madrid Train Bombing event, the FBI, which was considered as the most advanced institute in forensics, mistakenly located and arrested an innocent person whose name was Brandon Mayfield, because of a fingerprint misidentification. Induced by this tragic event, other wrong convictions and mistakes done by the FBI came to light, and eventually, the field of forensics received a negative impact. The US Congress ordered the National Academy of Science (NAS) to conduct research on the sciences used in Forensic Science. The main conclusion of work performed by the NAS was that there was *not too much science* in Forensic Science.[9]

In 2016, a Florida resident was arrested when an officer mistook a Krispy Kreme doughnut glaze for methamphetamine by having two false positive drug field tests. The long analysis time of seized drugs is a big challenge in U.S forensic labs. This creates backlog delays on evidence processing and innocent people may be waiting in jail. These erroneous incidents demonstrate the limitation of current forensic crime labs.

Nowadays, drug abuse is a growing global problem, leads to crime and health risk. In 2015, 29.5 million people—or 0.6 percent of the global adult population—were engaged in use and suffered from drug use disorders, including dependence. There is an increasing number of designer drugs. Designer drugs means a structural modification or functional analogue of listed illicit drugs, which can avoid legislative control. The number of new reported substances had nearly doubled to 483 compared with 260 designer drugs in 2012[10]. The growing number of designer drugs represent a challenge due that the majority of drug identification is done based on IR and MS databases. These databases fail to identify the all the new drugs. Furthermore, forensic labs do not have the resources to perform a full characterization of these designer drugs.

2. Current Methodologies in Drug Analysis

Current techniques used in the analysis of seized drugs are listed in table1 below[11]:

Table 1 Current analytical techniques in the analysis of seized drugs.

Category A	Category B	Category C
IR MS NMR Raman X-Ray Diffractometry	CE, GC, LC, IMS, Microcrystalline Tests, Pharmaceutical ID, TLC, Cannabis only: Macro Examination Micro Examination	Color Test Fluorescence Immunoassay Melting point UV

Category **A** techniques are considered as confirmatory techniques, category **B** techniques are considered as screening technique and category **C** techniques are considered as presumptive technique. The Scientific Working Group for the Analysis of Seized Drugs (SWGDRUG), has established recommendations to guide the drug analysis in Forensic Chemistry in 2011. In the recommendations, current analytical instruments were categorized into three main groups: Category **A** which are confirmatory, category **B** which are screening and category **C** which are presumptive. In order to obtain a minimum positive identification of seized drugs, one category **A** plus one category **B** or **C** are required. In 2017, these SWGDRUG recommendations were approved to become an ASTM standard for drug analysis. In the next section, currently utilized instruments in forensic chemistry will be discussed.

2.1 Mass Spectrometer and Ionization techniques

2.1.1 Mass Spectrometry

In the simplest terms, mass spectrometry contains two parts: ion source and a mass analyzer. The ion source generates gas-phase ions from analytes—organic or inorganic. These ions are separated by their different mass-to-charge ratios (m/z) and then detected qualitatively or quantitatively by their respective m/z and abundance. The analytes can be ionized by electrons, photons, excited atoms, or electrostatically charged droplets. Ions can consist of single ionized atoms, clusters, molecules, or their fragments or associates, depending on the ionization method. In a mass analyzer, ion separation is affected by electric and magnetic fields. These diverse types of ion sources and mass analyzers are based on different principles and therefore have different performance characteristics adapted to different scenarios and needs. Hybrid apparatus can combine those different performance characteristics offered by various types of mass analyzers into one mass spectrometer to provide unique applications for different fields of research.

Today, MS is mostly under the purview of the analytical chemistry field. In 1886, Eugen

Goldstein discovered that tubes with a perforated cathode emit a glow at the cathode end. Goldstein concluded that in addition to the already-known cathode rays—later recognized as electrons moving from the negatively charged cathode toward the positively charged anode—there is another ray that travels in the opposite direction. Because these latter rays passed through the holes, or channels, in the cathode, Goldstein called them Kanalstrahlen, or canal rays.[12] Canal rays were composed of positive ions which were converted from the residual gas inside the tube. Wilhelm Wien, a student of Hermann von Helmholtz, found that strong electric or magnetic fields deflected the canal rays, and in 1899 he constructed a device with parallel electric and magnetic fields that separated the positive rays according to their charge-to-mass ratio (Q/m).[13] Wien found that the charge-to-mass ratio depended on the nature of the gas in the discharge tube. In the 1900s, Wien's work was improved by J. J. Thomson who heightened the vacuum inside the tube and created the mass spectrograph.[14] Thomson's device was able to actually measure Q/m of the particles (electrons) that comprised cathode rays, which indirectly determined the mass of an electron.[15]

Developments of mass spectrometers continued over several decades leading to the discovery of new isotopes, as well as their accurate masses and relative abundances.[16] By the 1940s, chemists realized mass spectrometry's potential and it was established as an analytical tool, mostly for quantitative analysis.[15] Time-of-flight (TOF) mass analyzers were developed in 1946. Other developments of mass analyzers include ion cyclotron resonance (ICR) in 1948,[16] quadrupole and ion traps in 1953,[16] and orbitrap in the 2005.[17] Michael. A. Baldwin and Fred. W. McLafferty started to coupled HPLC with mass spectrometers in the 1970s. Their goal was to combine sample separation and mass analysis.[18]

Typically, in a mass spectrometry experiment, a sample, which could be solid, liquid, or gas, is ionized by an ion source. These ions are then separated by their different mass-to-charge (m/z) ratio. The ions are detected by a mechanism capable of detecting charged particles. Results are displayed as a spectrum of the relative abundance of ions detected as a function of the mass-to-charge ratio. The atoms or molecules in the sample can be identified by correlating known masses to the identified masses or through a characteristic fragmentation pattern. A significant breakthrough in the analysis of drugs, poisons, and/or their metabolites in body samples was the introduction of hyphenation techniques of chromatographic procedures with mass spectrometers.

2.1.2 Quadrupole Mass Analyzer

A quadrupole mass analyzer is a combination of four hyperbolically or cylindrically shaped rod electrodes extending in the z-direction and mounted in a square configuration (Figure 1).[19] The pairs of opposite rods (A and A or B and B) are each held at the same potential which is composed of a direct current and an alternating current component.

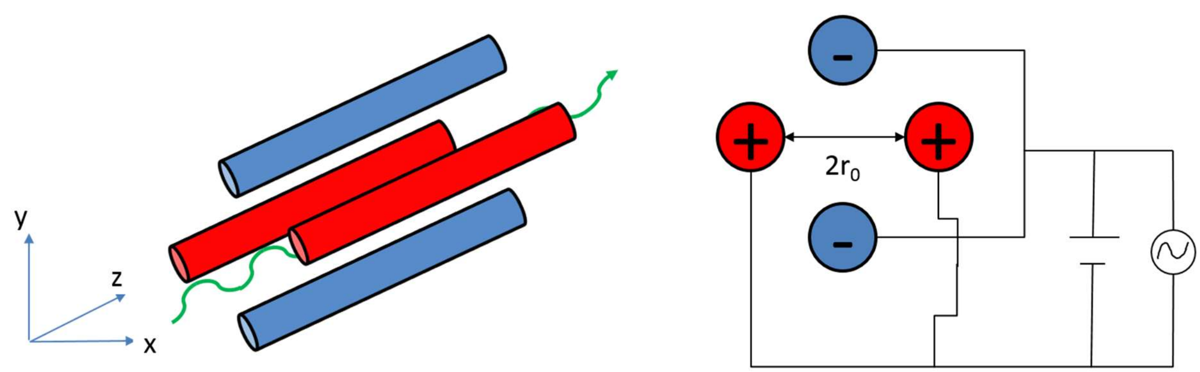

Figure 1 Cross section of a quadrupole for the cylindrical approximation.

As a mass analyzer, quadrupoles operate with both radio frequency (RF) and direct current (DC) voltage components applied to the rods. The reduced Mathieu parameters q_M and a_M are used to characterize the amplitudes of both components:[20]

$$q_M = \frac{4eV}{(m/z)\omega^2 r_0^2}, \quad a_M = \frac{8eU_{dc}}{(m/z)\omega^2 r_0^2} \quad (1)$$

where e is the charge of an electron, V and ω are the amplitude and angular frequency of the RF voltage, respectively. U_{dc} is the value of the DC voltage, and r_0 is the inscribed radius of the quadrupole. Under normal (mass-analyzing) operational conditions, only ions within a narrow m/z window are transmitted. This is the RF-only operational mode (a_M=0). Quadrupoles can also serve as either high-mass or low-mass filters for ions with m/z values above or below a certain cut-off value, depending on how the voltages are tuned.[21]

2.1.3 Time-of-Flight Mass Analyzer

The first time-of-flight (TOF) mass analyzer was developed in 1946 by William. E. Stephens.[22] A TOF operates under a simple principle demonstrated by its conspicuous long flight tube: ions are accelerated at the same time by an electric field with acceleration voltage U_a into the long flight tube, a field-free region. Potential energy obtained from U_a are equal among all ions and will be converted to kinetic energy (KE):

$$\mathrm{KE}=\frac{1}{2}mv^2 \quad (2)$$

where m is the mass and v is the velocity. Since mass and velocity are inversely proportional, the smaller the mass the faster the ion travels. Therefore, the lower mass ions will arrive at the detector earlier than the higher mass ions.

To compare two ions with different m/z, they must be accelerated at same time or a sufficiently short time interval. This is a difficult demand and brought forth the advent of the pulsed ion source, which can be realized either by pulsing ion packages out of a continuous beam or more conveniently by employing a true pulsed ionization method.[19]

Early TOFs were linear, which means ions are accelerated towards the flight tube to enter into a field-free region where they separated by their velocities before reaching the detector positioned at the other extremity of the flight tube. This linear TOF has a low resolving power due to initial spreads in the time, space and kinetic energy (KE) distributions of ions. (This applies only when U_a is constant, which is known as continuous extraction). Higher values of U_a (10-30 kV) minimize the contribution of the KE spread, but other factors still limit the resolving power (Figure 2 shows the effects and reasons).[23]

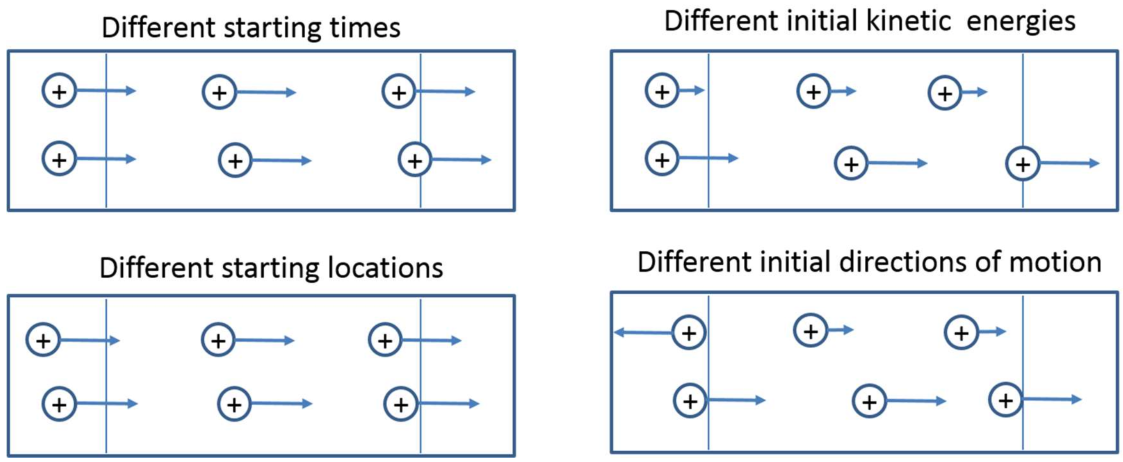

Figure 2 Effects of initial time, space, and kinetic energy distributions on mass resolution in TOF-MS.[23]

To improve the resolving power of TOF, Mamyrin devised the reflectron in 1994.[24]The reflectron acts as an ion mirror that focuses ions of different kinetic energies in time. A simple reflectron consists of a retarding electric field located behind the field free drift region opposed to the ion source. In practice, a reflectron is comprised of a series of ring-shaped electrodes at increasing potential. The reflection voltage U_r is set to about 1.05–1.10 times the acceleration voltage U_a in order to ensure that all ions are reflected within the homogeneous portion of the electric field of the device (Figure 3). The ions penetrate the reflectron until they reach zero kinetic energy and are then expelled from the reflectron in the opposite direction. The kinetic energy of the leaving ions remains unaffected, however, their flight paths vary according to their differences in kinetic energy. Ions carrying more kinetic energy will fly deeper into the decelerating field, and thus spend more time within the reflectron than less energetic ions. Thereby, the reflectron effects a correction in time-of-flight that substantially improves the resolving power of the TOF analyzer.[23,25-27] In addition, the reflectron provides focusing with respect to the angular spread of the ions leaving the source and it corrects for their spatial distribution.[24,26] Adjusting the reflectron at a small angle with respect to the ions exiting from the source allows the reflectron–detector to be placed adjacent to the ion source (Mamyrin design).[28]

The ability of the reflectron to compensate for the initial energy spread of ions largely increases the resolving power of TOF. The resolution of a reflectron-TOF is better than a common linear TOF.

Figure 3 Principle of operation of the reflectron.

After the development of reflectron, the TOF has the following advantages: 1. High mass range, according to its principle, the m/z range is unlimited;[29] 2. Fast scanning, complete mass spectrum is obtained within several microseconds; 3. High sensitivity; 4. The TOF instrument design and construction is comparatively simple and inexpensive to an ICR and orbitrap; 5. Recent instruments allow for accurate mass measurements and tandem MS experiments.[30]

2.1.4 Triple Quadrupole Mass Spectrometry

A hybrid mass spectrometry involves three quadrupole mass analyzer was developed in the 1970s.[31] This tandem mass spectrometry (MS/MS) features ion isolation and fragmentation which allows structural elucidation in depth. In addition, the most widely used function with a triple quadrupole mass spectrometry is its monitoring of MS/MS experiments. Both Selected Reaction Monitoring and Multi Reaction Monitoring opened the door to let researchers monitor a precursor ion and its specific product ions together with the ion abundance ratio at the same time.[32-34] Figure 4 below shows the schematic of a triple-quadrupole mass spectrometer.

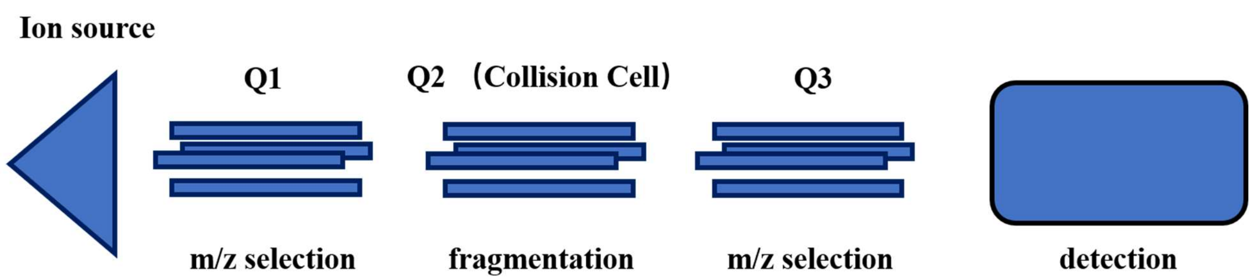

Figure 4 Triple-quadrupole mass spectrometer schematic.

Due to its excellent selectivity and sensitivity, selected reaction monitoring (SRM) mode analysis using triple quadrupole mass spectrometers (TQ-MS) has been the technology of choice for quantitation of small molecules in biological matrices.[35-37] In clinical labs, it has become the standard approach for liquid chromatography/mass spectrometry (LC/MS)-based quantitation. However, this approach requires optimization of tandem mass spectrometric (MS/MS) parameters for each compound to be analyzed. Compound optimization includes, at a minimum, selecting appropriate precursor/product ions and optimization of collision energies used for collision-induced dissociation (CID). This process is normally performed manually by introducing compound solutions into the mass spectrometers. Despite the many attempts at automation,[38-40] the SRM optimization still remains a discrete and time-consuming step in the development of a quantitative method. These processes typically require a dedicated and skilled analyst that will take into account possible crosstalks, adducts, unspecific ion transitions, etc.[41] Endogenous matrix interference with a similar m/z value can also be problematic.[42,43] Metabolites with a very close m/z value to that of the analyzed parent drug can also be problematic in SRM acquisition[44] and can possibly be resolved by high-resolution accurate mass (HR) acquisition[45].

Moreover, the selective nature of SRM acquisition can mask valuable information such as co-eluting matrix ions, degradation products or adducts of the analytes of interest. It can have a significant impact on assay quality and robustness when running a large number of various samples in a routine manner. The main advantages of HR over SRM acquisition in quantitative-qualitative (Quan-Qual) analyses have already been described. [45]

2.1.5 Q-TOF Mass Spectrometry

As a combination of high sensitivity and high mass accuracy for both precursor and product ions in both MS and tandem MS modes, quadrupole–time-of-flight (Q-TOF) mass spectrometers have been widely accepted by scientific community as powerful and robust instruments with unique capabilities with ion sources such as electrospray ionization (ESI), matrix-assisted laser desorption ionization (MALDI) and atmosphere pressure chemical ionization (APCI).

Schematic of a Q-TOF is presented in Figure 4. Samples are ionized from an ambient ion source, such as ESI or APCI, and ions travel through an ion guide (Figure 4) into a quadrupole, where ions can be selected for tandem mass spectrometry experiments at the collision cell. The octopole ion guide helps to focus on the ions entering the instrument and as well as the hexapole. Octopole and hexapole provide both radial and axial collisional damping of ion motion. The ions are thermalized in collisions with neutral gas molecules, reducing both the energy spread and the beam diameter and resulting in better transmission into and through both the quadrupole[46] and TOF[47] analyzers. After leaving the hexapoles, ions are re-accelerated in the axial direction to the necessary energies with near-thermal energy spreads.

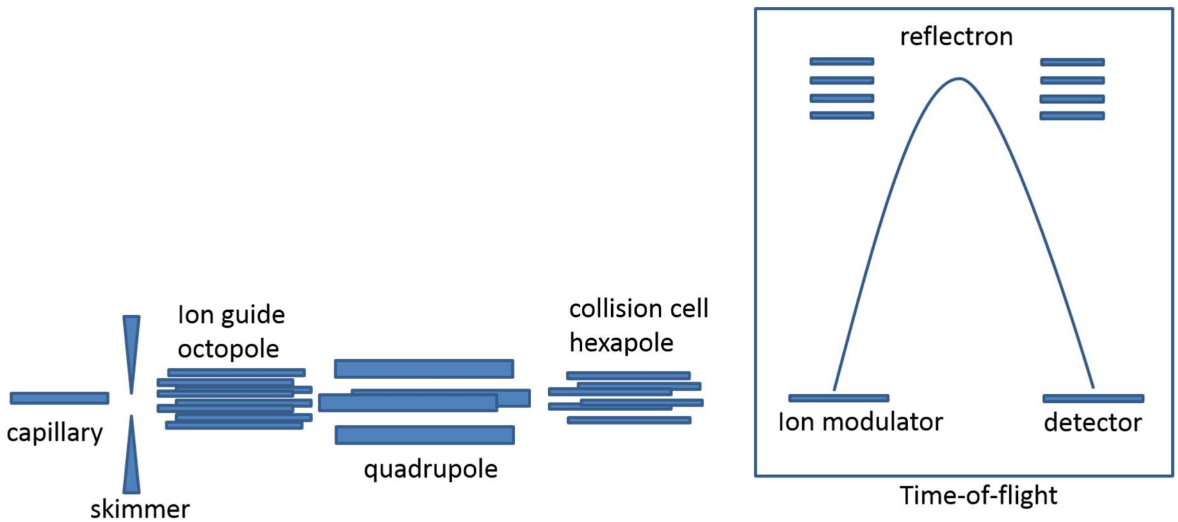

Figure 5 Quadrupole time-of-flight mass analyzer schematic

For MS/MS, the quadrupole is operated in the mass filter mode to transmit only the parent ion of interest. The target ion is then accelerated before it enters the collision cell (hexapole), where it undergoes collision-induced dissociation (CID) after the first few collisions with neutral gas molecules (usually argon or nitrogen). The resulting fragment ions (in addition to the remaining parent ions) are collision-cooled and focused towards the TOF analyzer and detected.

2.1.6 Electrospray Ionization

In 1984, Masamichi Yamashita and John Fenn developed electrospray ionization (ESI), a new ionization source. This soft method allows less fragmentation or even no fragmentation during ionization.[48] Now, ESI has become the most widely used ionization technique due to its ability to be applicable for a vast variety of analytes such as inorganic and organic compounds. Due to its multiple-charged feature, polymers, lipids, peptides, and proteins with high molecular mass are able to be ionized. In addition, ESI allows coupling with liquid chromatography enhancing the field of MS analysis.

During the ESI process, three major steps are required to generate ions in gas from electrolyte solution: (a) The production of charged droplets at the electrospray capillary tip; (b) Shrinkage of the charged droplets due to solvent evaporation and Rayleigh fissions (also called Coulomb fission); (c) the actual mechanism by which gas phase ions are produced from these droplets. The stages (a) to (c) occur in the atmospheric pressure region of the apparatus (see Figure 5).

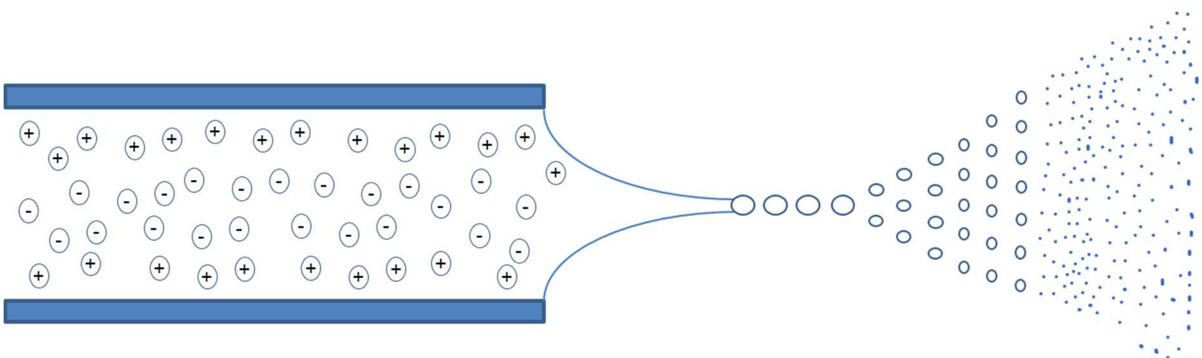

Figure 6 Illustration of major processes in the atmospheric pressure region of an ESI ion source run in the positive ion mode.

In positive mode, the electric field, which is near the spray capillary tip, will polarize the solution. Under this polarization influence of the electric field, the solution will be sufficiently conducting. Then the positive ions in the solution will move to the surface of the meniscus and negative ions will move away from the meniscus. The downfield forces due to the polarization cause a distortion of the meniscus into a cone pointing downfield. The increase of surface due to the cone formation is resisted by the surface tension of the liquid[49]. This liquid cone is named as Taylor cone.[50] The liquid cone tip becomes unstable if the electric field is high enough. Therefore, a fine jet emerges from the cone tip. The surface of the jet is charged by an excess of cations. The repulsion between the charges on the jet causes the jet to break up into small charged droplets.[51]

The charged droplets will then shrink due to solvent evaporation while the charge remains constant. The energy required for the solvent evaporation is provided by the thermal energy of the ambient gas, air at atmospheric pressure in most cases. As the droplet gets smaller the repulsion between the charges at the surface increases, and at a certain droplet radius, this repulsion overcomes the cohesive force of the surface tension. An instability results and leads to fission of the droplet that typically releases a jet of small, charged progeny droplets. The condition for the instability, also called Rayleigh fission or Coulomb fission, is given by the Rayleigh equation[52]:

$$Q_{Ry} = 8\pi(\varepsilon_0 \gamma R^3)^{\frac{1}{2}} \qquad (3)$$

where Q_{Ry} is the charge on the droplet, γ is the surface tension of the solvent, R is the radius of the droplet, and ε_0 is the vacuum permittivity.

Droplets at constant charge will experience the Rayleigh fission at or near the Rayleigh limit which is provided by equation (3), and then emit a jet of small, monodisperse charged product droplets. This shrinkage process has been confirmed by a number of experiments.[53-55] The loss of mass on fission is less than 1% of the parent droplet but the loss of charge is much larger, that is, some 15–25% of the charge of the parent droplet.[56]

Having repeated Rayleigh fissions, the parent droplets become smaller and smaller and eventually will convert to very small charged droplets which are the precursors of the gas-phase ions. The mechanisms by which the gas phase ions are produced from the very small “final” droplets is still not cleared. Two main assumptions are provided.

Malcolm Dole developed the charge residue model (CRM) in 1968.[57] The CRM assumes that the surface area of parent droplets decreases due to collisions with heated drying gas and/or heated capillary. Figure 6 presents the CRM.

As the parent droplet reduces in size, the charges on the surface move closer together, this results in Rayleigh fission. The offspring droplets that are formed from the parent droplet further reduce in size through the evaporation of solvent molecules. Each offspring droplet contains one analyte molecule. As the solvent molecules evaporate from the offspring droplets, the charge is deposited onto the surface of the analyte, thus producing gas-phase ions. The CRM applies by default to large molecules (MDa) since each droplet is only able to contain one molecule.

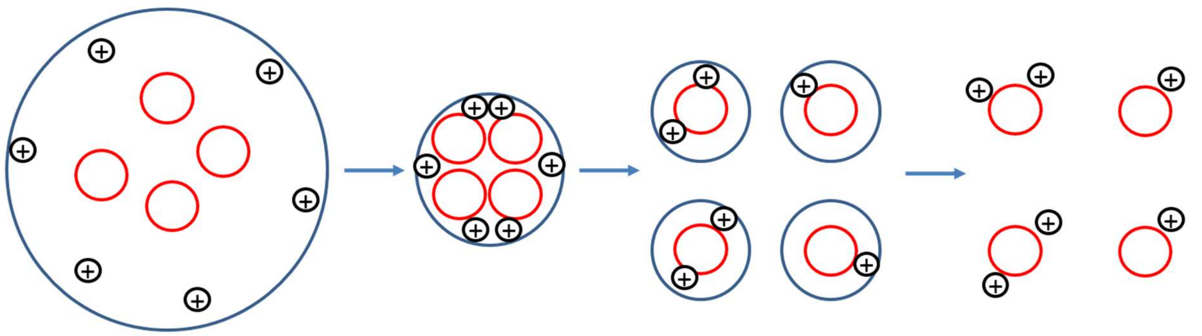

Figure 7 Charge residue model schematic.

The Charged Residue Mechanism works well for macromolecules. It has allowed quantitative predictions of the protein charge state in the gas phase using a simple correlation between charge state and protein mass and is well supported for proteins of widely varying mass.[56]

The ion evaporation model (IEM) was proposed by Iribarne and Thomson in 1976.[58] Like the CRM, the IEM assumes the evaporation and dissociation of parent droplets into offspring droplets. As the radius of the offspring droplet continues to decrease, the charge density and electric field increase.[16]The surface charge density is sufficiently lower than the Rayleigh limit, which causes the ejection of an ion from the offspring droplet instead of droplet dissociation. Figure 7 presents the IEM schematic. In MS experiments, the IEM is well-supported for small ions.[59] However, unlike the CRM, it does not apply for very large ions.

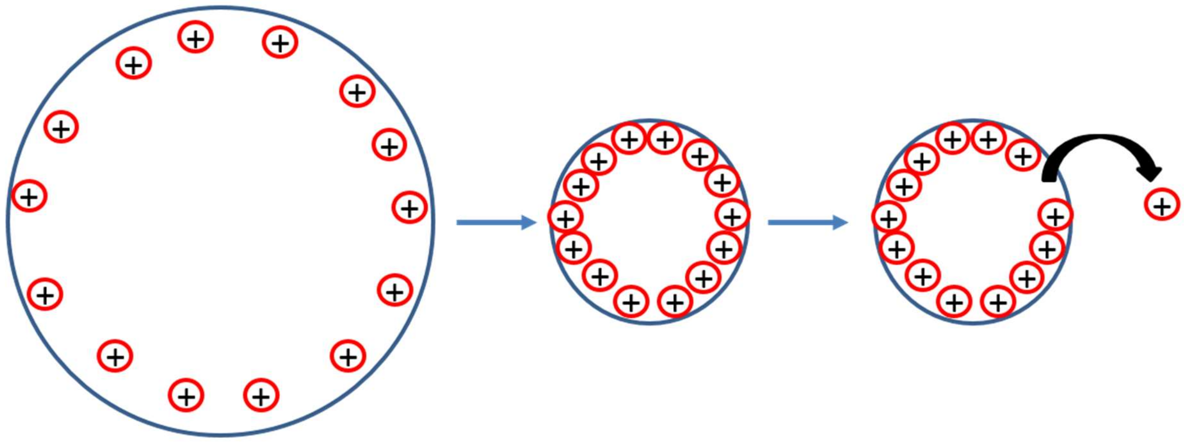

Figure 8 Ion evaporation model schematic.

As a summary, the real mechanism is possibly a combination of CRM and IEM. The authors propose that the lower charge states are due to an ion evaporation stage (IEM) that precedes the charged residue formation (CRM) of the protein.

2.1.7 Direct Analysis in Real Time (DART)

In 2005, DART mass spectrometry was developed to bring the possibility to perform rapid, non-contact analysis of materials at ambient pressure and with zero sample preparation.[60,61] In 2006, a first report demonstrates the potential of DART to screen tableted antimalarials for counterfeits.[62] In addition, the potential of DART mass spectrometry for monitoring the quality of tableted medicines was published.[63,64] In DART, samples are subjected to gas-phase ionization processes shares similarities to the gas phase ionization processes in atmospheric pressure chemical ionization (APCI)[65,66] or atmospheric pressure photoionization (APPI).[67,68] Helium or nitrogen atoms which were excited by DART would release into the atmosphere to initiate the gas-phase ionization. Thus, atmospheric water vapor or other gaseous compounds would be ionized by the excited gas to create reagent ions. Then, these reagent ions promote chemical ionization of the analyte. Due to its mechanism, Compounds with high molecular weight and nonvolatility are infrequently ionizable when using DART. Since these compounds are usually the potential interference in the matrix, the absence of them became a major advantage of DART. Figure 8 shows the scheme of DART. The mechanism of ionization of DART using helium or nitrogen is described on the equations below:

$He + energy \rightarrow He^*$ (1)

$He^* + N_2 \rightarrow He + N_2^+ + e^-$ (2)

$He^* + M \rightarrow He + M^+ + e^-$ (3)

$N_2^+ + H_2O \rightarrow H_2O^+ + N_2$ (4)

$N_2^+ + M \rightarrow M^+ + N_2$ (5)

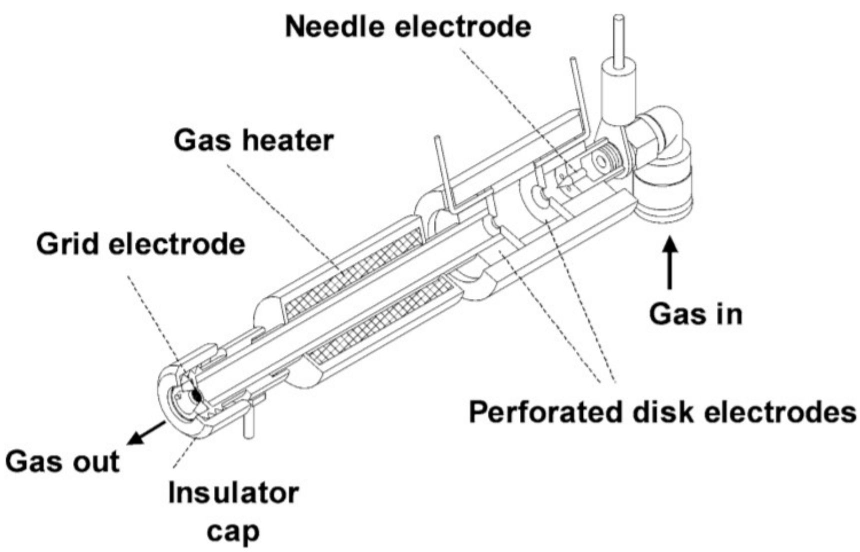

Figure 9 Schematic diagram of DART.[60]

In February 2007, the Virginia Department of Forensic Science couple DART with a JEOL, Inc. (Peabody, MA) AccuTOF accurate mass spectrometer, online for development as a screening and confirmation tool in the analysis of drugs of abuse. Screening and confirmation of solid dosage forms of drugs are done by color tests, thin layer chromatography, and time-consuming temperature-programmed runs on a gas chromatograph-mass spectrometer. Because the DART ionization technique was relatively new and untested in a forensic setting, a validation study needed to be carried out to determine the efficacy of the technique, with respect to these established analytical protocols. While the DART source produces spectra similar to other atmospheric pressure ionization techniques, especially electrospray ionization, differences would be expected due to the manner in which ions are produced.

In general, DART ionization produces spectra with a characteristic peak at the protonated or deprotonated molecule. These ions are measured at their exact mass in the AccuTOF mass spectrometer. Elemental composition calculations, based on empirical formulas, can be performed on these ions to determine whether they fall within a specified error, usually measured in millimass units (mmu), of a known compound.

While accurate-mass spectra have an inherent specificity, confirmation is difficult if the possibility of an isomer exists. In order to be used as a confirmation step in a drug analysis scheme, it is important that the DART spectra have characteristic peaks that can be used to confirm the presence of the suspected drug compounds. By varying the voltage on the orifice 1 of the AccuTOF, spectra with extensive fragmentation can be produced by in-source collision-induced dissociation (CID). Simultaneous collection of data at different orifice 1 voltages can be accomplished by utilizing the ‘‘function switching’’ mode of the AccuTOF operating software. Higher orifice 1 voltages generally result in more fragmentation and therefore more characteristic ions being produced. The combination of accurate mass measurement of the protonated molecule and characteristic CID fragmentation allows for the production of spectra that can be used as part of an identification scheme for drugs of abuse.

2.2 Separation with High Performance Liquid Chromatography (HPLC)

Most materials in our surroundings are mixtures of two or more components. Mixtures can be separated into their components by several physical methods. The choice of separation techniques is based on the type of mixture and difference in the chemical properties of the components of the mixture, such as polarity, size, H-bonding or π-π interaction. Depending on these involved properties, chromatography can be classified into five modes of separation based on the interaction between the stationary and mobile phase: adsorption (normal-phase), partition, ion exchange, molecular exclusion (size exclusion), and affinity chromatography.

Chromatography is a separation technique used to separate the different components in a liquid mixture. It was introduced by Michael Tswett.[69] Chromatography involves the sample being dissolved in a particular solvent called mobile phase. The mobile phase can be liquid or gas. The mobile phase is then passed through another phase called the stationary phase. In this process, the different properties of components lead to different interaction with both mobile phase and stationary phase. The various components of the mixture travel at different speeds, causing them to separate. There are different types of chromatographic techniques such as column chromatography, thin layer chromatography, paper chromatography, gas chromatography(GC) and liquid chromatography (LC).

Generally, LC is coupled with a diode array detector (DAD).[70] The UV and visible light absorption of the sample are continuously measured at single or multiple selected wavelengths.

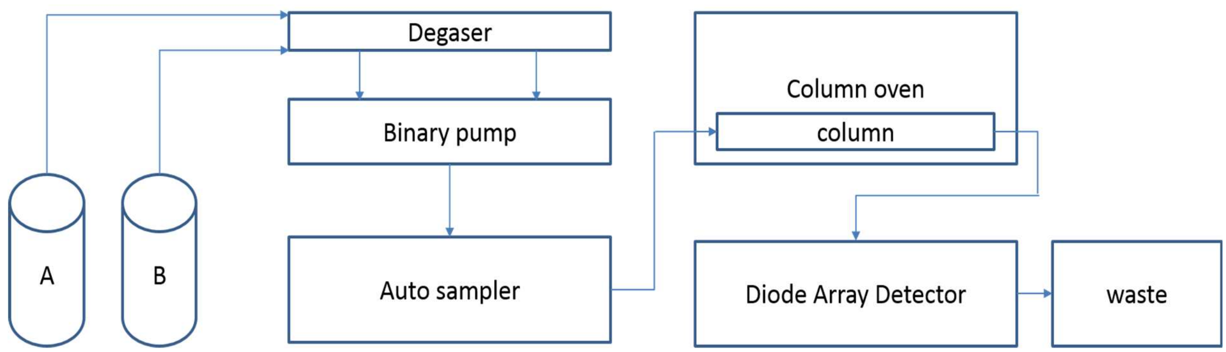

Figure 10 HPLC schematic.

The typical LC system contains mobile phase reservoirs, a degasser, pump, auto-sampler, column and column oven, and detector. Figure 9 presents a schematic of an HPLC system. The LC system used in this experiment utilizes a Reverse-phase liquid chromatography (RPLC) method. RPLC is one of the most popular modes of separation used in chromatography. In normal-phase chromatography, the stationary phase is polar and the mobile phase is non-polar. RPC is the reverse of normal-phase chromatography, hence the name. The stationary phase is non-polar and the mobile phase is polar. Typical stationary phases consist of long hydrocarbon chains, such as octadecyl (C18), octyl (C8), and phenyl, attached to a support (silica or cross-linked polymer), while the mobile phase uses polar solvents such as methanol, acetonitrile, and tetrahydrofuran (THF). These solvents are typically mixed with water.[71]

In clinical and forensic science, all impartial toxicological judgments and proper consultations are based on robust and reliable qualitative and quantitative analysis. But in most cases, the expect analytes are not well-known in advance and many other interfering biomolecules may negatively impact their detection, especially when analyzing in complex biological matrices such as post-mortem blood (plasma, serum), urine, saliva, tissues, or alternative matrices such as hair, nail, or sweat. Thus, separation techniques such as HPLC and GC coupled to a mass spectrometry had become the most famous analytical methodology in all fields of analytical toxicology owing to its high identification and separation power combined with high sensitivity. As a combination of the physical separation, function of HPLC, with the mass analysis, function of MS. HPLC-MS gained its popularity on a variety of aspects and applications.

2.3 MicroFluidics

In the past a few years, microfluidic technologies have become famous in multiple research aspects due to the unique outstanding benefits such as their small sample amount requirement, the reduction in the solvent amount used, waste production and fast analysis speed, as well as the lower energy utilization.[72] Thus, microfluidics has attracted interests in forensic science[73] especially on explosives analysis, blood test[74] and drug analysis.[75-78] Increasing number of researchers have developed different microfluidic platforms for various purposes as drug extraction,[79] screening,[80] and detection[81].

Other studies have focused on microfluidics devices that can be used for presumptive testing of illicit drugs. These devices focus on separation, extraction, and quick screening and preliminary identification of drugs such as amphetamines, cocaine, morphine, methamphetamine, barbiturates, and benzodiazepines.[82-84]

The first microfluidic system utilized for drugs of abuse analysis was described in 2000 by Greenway et al.[85] The platform was based on the use of $Ru(bipy)_3{}^{2+}$ chemiluminescence (CL) to detect codeine. Since then, numerous different and more complex systems have been reported.

Other studies have focused on microfluidics devices that can be used for presumptive testing of illicit drugs. These devices focus on separation, extraction, and quick screening and preliminary identification of drugs such as amphetamines, cocaine, morphine, methamphetamine, barbiturates, and benzodiazepines.[82-84]

Immunoassays are the first screening tests performed for forensic drug analysis in biological samples. Through a specific molecular recognition, an antibody and antigen bind to form an antibody-antigen complex. In this complex, either the antibody or antigen is labeled, which enables the detection and quantification of trace amounts of the drug.[86]

Extraction of a drug from a biological sample, such as a bodily fluid or tissue, is the first step in the confirmatory drug analysis. The sample is usually subjected to one of the two common extraction techniques—SPE or liquid–liquid extraction (LLE)—to eliminate the matrix effect and pre-concentrate the drug.[87-89] In microfluidics, in addition to SPE and LLE, more extraction ideas have been tested.

Following the extraction of the drugs, separation is commonly performed using GC or HPLC. Although these are the two most popular separation techniques in forensic laboratories[90], the emphasis in microfluidic drug separation was on electrokinetic methods, including CE and MEKC.

Recently, Drs. Dow, Hinks, and Vinueza from NC State University developed a new microfluidic device (MFD) for the extraction of dyes from fibers of “forensic size” (~1 mm in length) under NIJ grant 2011-90824-NC-DN. This device has a cavity that can be used for other purposes such as paper, fibers, or paper containing dry blood spots (DBS). The scheme of microfluidics is presented in Figure 10. Figure 11 and Figure 12 demonstrate the design of the microfluidic cavity chip and how to place the sample onto the chip. Trace amount sample could be easily put onto the sample holding post. During extraction, the solvent will be introduced through the fluid inlet. After extraction, the extracted solution will be pushed out through the fluidic inlet. Nitrogen gas is applied as a driving force.

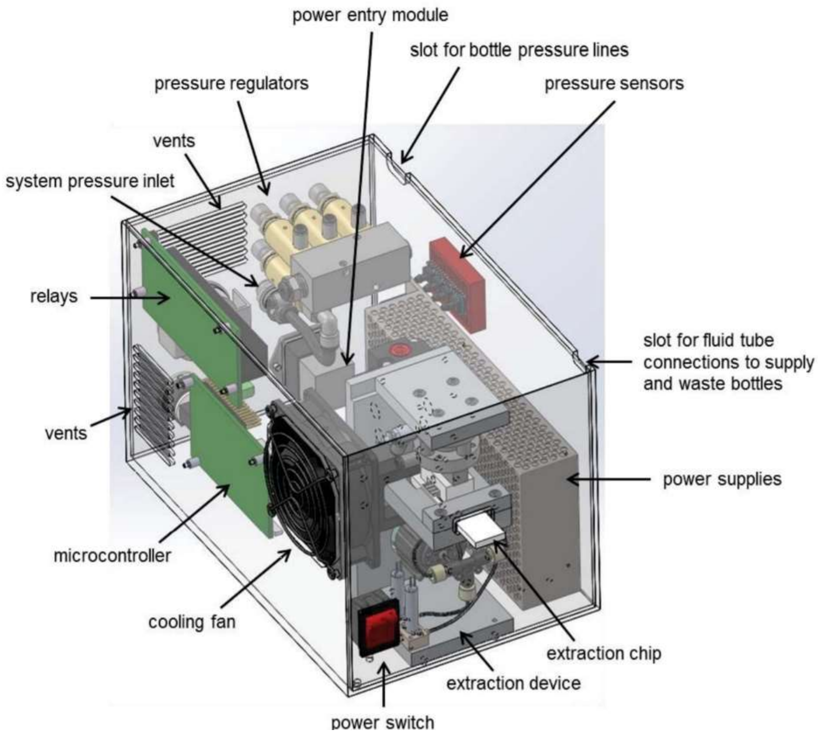

Figure 11 Schematic diagram of the Microfluidic Device.

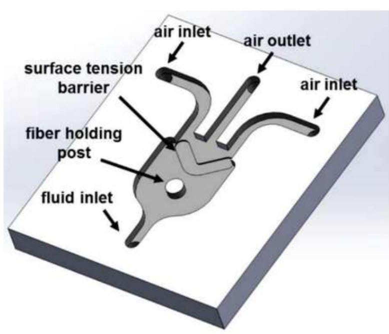

Figure 12 Design of microfluidics cavity chip.

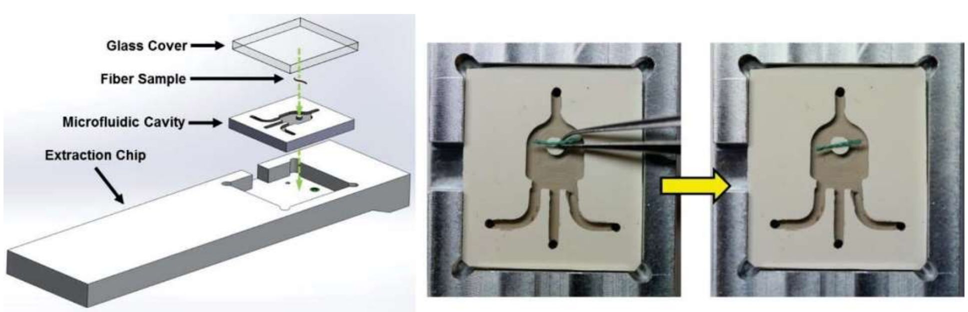

Figure 13 Sample placement onto cavity chip.

The extracted material can be collected for chromatography and mass spectrometry analysis. However, this process can be avoided if the MFD can be connected directly to a mass spectrometer for a faster analysis.

2.4 Sample preparation methodologies

2.4.1 Solid Phase Extraction

As the most widely used sample preparation method, solid-phase extraction (SPE) is used by analytical laboratories to purify or concentrate target analytes from a complex mixture of samples for analysis. In an SPE procedure, the sample needs to be dissolved or suspended in a solvent, then passed a solid phase through to get a separation among multiple components. Depending on the samples and SPE materials, the target analytes of interest may be either in the eluted solution or retained in the solid phase. If the target analytes retained in the solid phase, an extra step of elution with suitable solvent is needed to obtain the analytes from the solid phase for future analysis.

Commercial miniaturized Solid Phase Extraction(SPE) devices are available in a variety of formats and are currently widely utilized in many crime labs for forensic purpose. Solid-phase extraction is now the most form of removing drugs from biological fluids prior to analysis (HPLC, GC, GC/MS, etc.). The economic reasons behind the use of solid-phase columns have been well documented and include markedly reduced solvent consumption (and therefore reduced solvent disposal), faster laboratory turnover time, increased extraction efficiency, no emulsion formation, decreased evaporation volumes, and ease of automation compared to traditional solvent extraction procedures. Different types of solid phase materials are available such as normal phase, reverse phase, ion exchange, etc. SPE is a relatively cost-effective methodology because it is reusable and the reconditioning process is easy to operate.

SPE also has various branched techniques such as Micro Extraction by Packed Sorbent (MEPS), this combination of SPE cartridge and a syringe has a sorbent bed inserted into the barrel of the syringe. In the MEPS procedure, the liquid sample is aspirated and ejected multiple times using the MEPS syringe.

2.4.2 Solid Phase Micro Extraction

Solid Phase Micro Extraction (SPME) is a sample preparation methodology based on a coated fiber in the syringe. SPME was originally designed as a technique for the solvent-free analysis of volatile organic contaminants in environmental samples. The fiber is a solid support which coated by a dispersed material which plays the role as an extracting phase. During headspace sampling which was first described in 1993, the fiber is exposed to the sample for a period of time to absorb volatile analytes. Then the fiber is heated to desorb the analytes for GC analysis. The ease of operation is an obvious advantage of SPME. Besides this, SPME presents excellent LOD and LOQ.[89,91]

Thus, a wide variety of applications are now being pursued, including the analysis of drugs from a variety of biological and related matrices, including blood, plasma, urine, hair, and saliva. SPME offers the potential for very 'clean' analyses, with little to no interference from non-volatile compounds. Most of the reported methods shown to date have involved headspace techniques for volatile drugs with excellent selectivity. However, the current limitation is sample type and time consumption. Since SPME requires a volatile sample, sometimes the non-volatile samples need to be derivatized. The entire SPME process also requires very long sample preparation time (~60min), long desorption time (~20min) and needs to be re-conditioned every time (300 ℃ up to 120mins until no peaks appear in the GC).

Solid phase microextraction – microfluidic device (SPME-MFD) system was reported by Choi, K et al. This SPME-MFD device was coupled to LC-MS for confirmatory analysis. The LOD could be as low as 500pg/mL, but it requires a 60 min immersion time for sample preparation, and SPME fibers need to be re-conditioned every time.

2.5 Electrospun nanofibers

Electrospinning is a relatively new technique to produce continuous fibers with diameters down to a few nanometers. Both synthetic and natural polymers could be electrospun. In addition, other agents like metals particles, reactive agents and nanoparticles are possible to be blended and loaded with polymer to make special functionalized nanofibers. Because of its simplicity of processing, electrospinning technique is now increasingly being employed in university laboratories and industry.

Electronspun nanofibers gained popularity in various fields such as medical materials, special textiles, filtration techniques, and nano-electronics.[1,2,92,93] The advantage of using nanofibers is the high surface-to-volume ratio. The high surface-to-volume ratio makes nanofiber an outstanding material to be combined with MFD.

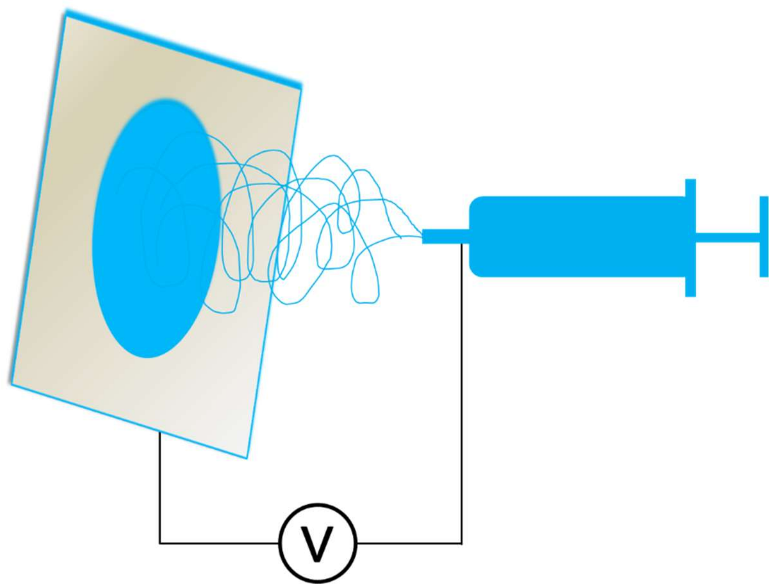

Figure 14 Schematic diagram of electrospinning.

The scheme of a typical electrospinning experiment in a laboratory is shown in Figure 13. In the beginning, the selected polymer solution is pumped through a needle. This needle also works as an electrode with a high electric field of 10-16 kV. On the other side, there is a piece of foil as nanofiber collector and the counter electrode. In typical laboratory uses, the distance between needle and foil is 10–25 cm. The currents that flow during electrospinning range from a few hundred nanoamperes to microamperes.

Once the high voltage applied to this system, it causes a cone-shaped deformation of the drop of polymer solution[50]. Then deformed drop will form a jet to flies towards the collector. During the flight, the solvent in the jet evaporates and polymers are eventually formed nanofibers and precipitated on the collector.[92,94] Therefore, a nanofiber mat could be obtained on the collector as a result of sustaining polymer solution injecting and high voltage. After cooling and drying, the nanofibers are then transferred to Scanning Electron Microscope (SEM) to the characterization of its microstructure.

3. Research Objectives

The goal of this research is to develop qualitative and quantitative analysis methods that allow for rapid, cost-effective drug screening using a microfluidic device coupled with a quadrupole-time-of-flight mass spectrometer for forensic applications. The methods also enable high throughput by eliminating lengthy sample preparation and chromatography.

Aim 1: Develop an MFD-MS method for fast screening and identification of drugs.

Produce nanofibers by electrospinning as drug adsorption substrate to provide a selective and rapid sampling for the microfluidic extraction, which will be coupled with a mass spectrometer for screening purposes.

Aim 2: Examine the selectivity of different nanofibers. by choosing nanofibers with different organic group functionalities.

Based on the hypothesis of the influence of intermolecular interactions, more nanofibers with different organic group functionalities are produced to obtain different surfaces with diverse intermolecular interactions. Comparing the elution profile of different drug mixtures and the results of computed molecular properties will help understand their selectivity.

Aim 3: Application on porcine plasma and method validation.

Apply the best method to a porcine plasma sample, which is a good alternative to human post-mortem blood, for forensic applications. Validate the quantitation method based on the U.S. Food and Drug Administration standards. Comparing the LOD and LOQ to North Carolina Office of the Chief Medical Examiner and other forensic articles recommended values. This recommended guide could be found on NCOCME Toxicology website.

4. Development of selective drug screening method using nanofibers via MFD-MS

4.1 Abstract

Drug abuse puts serious health risk on people no matter their ages and societies, and this global problem is growing even faster.[3] Nowadays, forensic labs have a lack of the resources, funding, and knowledge. The analysts are working with methods that rely on limited databases for identification that lack these new compounds. Current sample preparation methods for trace drug analysis are most commonly performed using solid-phase microextraction, or SPME requires long sample preparation time and re-conditioning time. Thus, accurate and rapid analytical systems are needed for drug screening and analysis in the forensic field. This study will discuss a methodology involves electrospun nanofibers, microfluidic extraction, mass spectrometry, the benefits of selectivity and rapid analysis.

4.2 Introduction

Forensic science is the application of science to criminal and civil laws during the investigation, governed by legal standards of admissible evidence and criminal procedure. Crime Scene Investigation Procedure contains collection, preservation, and analysis of scientific evidence. The diversity of professions practicing Forensic Science may be illustrated by the 11 sections of the American Academy of Forensic Sciences (AAFS) classification: Criminalistics, Digital and Multimedia Sciences, Engineering Sciences, General, Jurisprudence, Odontology, Pathology and Biology, Physical Anthropology, Psychiatry and Behavioral Sciences, Questioned Documents and Toxicology. Drug abuse puts serious health risk on people no matter their ages and societies, and this global problem is growing even faster.[3] In forensic drug analysis, according to their pharmacological effect, drugs could be classified as depressants, such as barbiturates and benzodiazepines; stimulants, such as amphetamines and cocaine; analgesics, such as opioids and psychotomimetics such as marijuana[4].

Unfortunately, forensic science is not as robust as society thought, Forensic Science has a "lack of science". In 2004 Madrid Train Bombing event, FBI, which was considered as the most advanced institute in forensic aspects, mistakenly located and arrested an innocent person whose name was Brandon Mayfield because of a fingerprint misidentification. Induced by this tragic event, other wrong convictions and mistakes of the FBI were mentioned, and eventually, the field of forensics received a negative impact. The US Congress ordered the National Academy of Science to conduct research of the sciences used in Forensic Science.

Therefore, as a result of the NAS report, the Scientific Working Group for the Analysis of Seized Drugs (SWGDRUG) recommendations were used to guide the drug analysis in Forensic Chemistry in 2011. In the recommendations, current analytical instrumentations were categorized into three main groups: Category A which is confirmatory, category B which is screening and category C which is presumptive. In order to obtain a minimum positive identification of seized drugs, one category A plus one category B or C are required. In 2017, these SWGDRUG recommendations were approved to become an ASTM standard for drug analysis. In the next section, currently utilized instrumentation in forensic science will be discussed.

Nowadays, forensic labs have a lack of the resources, funding, and knowledge. The analysts are working with methods that rely on limited databases for identification that lack these new compounds. Therefore, a large amount of evidence needs to be transferred to some third party labs to do the entire identification and characterization. All these increasing evidence analysis time. Thus, the long analysis time of seized drugs is a big challenge in forensic labs. This creates backlog delays on evidence processing and innocent people may be waiting in jail. These erroneous incidents demonstrate the limitation of current forensic crime labs. New methodologies need to be accomplished.

Current sample preparation methods for trace drug analysis are most commonly performed using solid-phase microextraction, or SPME. SPME uses a low-polar or non-polar coated fiber to absorb volatiles from solution without contact. The fiber is then heated to desorb the volatiles for GC analysis. The benefits of SPME includes the ease to operate and excellent limits of detection and quantitation (LOD and LOQ). Various researchers reported that they obtained the LOD could be as low as several tens or hundreds of pg/mL level, but the sample preparation time is 60-minutes long. In addition, the SPME fibers need to be re-conditioned for around 30-minute every time after use.

Thus, accurate and rapid analytical systems are needed for drug analysis in the forensic and pharmaceutical field. Drug abuse puts serious health risk on people no matter their ages and societies, and this global problem is growing even faster.[3] In forensic drug analysis, according to their pharmacological effect, drugs could be classified as depressants, such as barbiturates and benzodiazepines; stimulants, such as amphetamines and cocaine; analgesics, such as opioids and psychotomimetics such as marijuana[4].

Based on immunoassay technologies, certain on-site screening devices have been developed and became commercially available.[5-7] The first microfluidic system utilized for drugs of abuse analysis was described in 2000 by Greenway and his colleague[85] to detect codeine based on the use of $Ru(bipy)_3{}^{2+}$ chemiluminescence (CL). Since then, numerous different and more complex systems have been reported.

Other studies have focused on microfluidics devices that can be used for presumptive testing of illicit drugs. These devices focus on separation, extraction, and quick screening and preliminary identification of drugs such as amphetamines, cocaine, morphine, methamphetamine, barbiturates, and benzodiazepines.[82-84]

Mass spectrometry with high resolution offers great sensitivity and versatility, which in combination with microfluidics and liquid chromatography can be a unique analytical tool for both purposes. In addition, mass spectrometry methods coupled with separation techniques such as GC-MS and HPLC-MS have been utilized[8]. An ideal on-site drug analysis system should provide reliable qualitative and quantitative results with minimal sample preparation. Therefore, a multidimensional system for the drug analysis is needed to assist in the fast screening and identification.

In this study, the electrospinning technique was used to produce nanofibers. The high surface-to-volume ratio of nanofibers provided better adsorptive performance comparing with a cotton swab, as well as dramatically reduced time consumption comparing with SPME. A microfluidic extraction device coupled to an Agilent Q-TOF mass spectrometry allowed rapid extraction and MS analysis.

4.3 Materials

4.3.1 Solvent

HPLC grade acetonitrile and methanol were purchased from J.T.Baker, Deionized water was obtained from ELGA Purelab Ultra AN MK2.

Porcine blood with heparin was obtained from NC State University, College of Veterinary Medicine.

4.3.2 Other supplies

Disposable Luer-slip plastic syringes (1 mL), Millex-GV 13 mm, 0.22 μm polyvinylidene fluoride (PVDF) filters, syringe needles (0.52 mm O.D. x 0.26 mm I.D., 25 gauge), and Fisherbrand 15 x 45 mm, 1-dram glass vials were purchased from Fisher Scientific. Amber screw top glass vials (2 mL) were purchased from Agilent Technologies (Part number: 5188-6535).

4.3.3 Drug Standards

Drug standards M-025, O-020 and S-038 were purchased from Cerilliant Inc. An artificial drug mixture solution was obtained from Shimadzu via collaboration.

4.4 Experiments and instrumentation

4.4.1 Sample preparation

All drug standards were prepared for analysis by diluting in 1 mL of methanol in a 1-dram Fisherbrand 15 x 45 mm, glass vial to make the concentration of 100 ng/mL. Since most common drugs have recommended LOD around 100 ng/mL, according to the North Carolina Office of the Chief Medicine Examiner(NCOCME). The diluted samples were transferred into 2-mL Agilent amber screw top glass LC vials (Part number: 5188-6535) for analysis.

Porcine plasma was separated from porcine blood by using a centrifuge set at 2400 rpm for 10 min.

4.4.2 Nanofiber preparation by electrospinning

Polyacrylonitrile (PAN), polyvinylidene difluoride (PVDF), and polyvinyl alcohol(PVA) nanofibers were prepared for this study. These nanofibers were selected due to their structure (functionality) and ease of control of the fiber diameter during production. The preparation of the PAN nanofibers by electrospinning was performed by making a solution of 2.4 g of polyacrylonitrile (PAN, Mw = 150,000, Sigma–Aldrich) and mixing it with 30 g of N,N-dimethylformamide, followed by mechanical stirring at 50 °C for 24 h. The solution was transferred to a syringe and was electrospun into nanofibers under a high voltage of 15 kV. During electrospinning, the needle-collector distance and the feed rate were fixed at 15 cm and 0.75 mL/min, respectively. For PVDF nanofibers, preparation of a solution of N,N-Dimethylacetamide/acetone (7:3) was mixed with polyvinylidene fluoride (PVDF, MW = 400,000, Sinopharm Chemical Reagent Co., Ltd) to obtain a 12% wt. solution, which was stirred at 60°C for 12 h. The solution was transferred to a syringe and was electrospun into nanofibers under a high voltage of 16 kV. During electrospinning, the needle-collector distance and the feed rate were fixed at 20 cm and 0.4 mL/h, respectively. For Chitosan nanofibers, preparation of a solution of acetic acid (90% aqueous) was mixed with chitosan (MW = 190,000, Sigma–Aldrich) to obtain a 5% wt solution, which was stirred at 25°C for 12 h. The solution was transferred to a syringe and was electrospun into nanofibers under a high voltage of 16 kV. During electrospinning, the needle-collector distance and the feed rate were fixed at 10 cm and 0.4 mL/h, respectively.

After preparation, PVA and Chitosan nanofibers were then transferred into the oven to be heated for 4 hours to get crosslinked. This process is necessary to avoid dissolution in water.

4.4.3 Mass Spectrometry

MS: The Agilent Technologies 1260 liquid chromatography is coupled to an Agilent Technologies 6520 Accurate-Mass Quadrupole–Time-of-Flight (Q-TOF) mass spectrometry equipped with an electrospray ionization (ESI) source or direct analysis in real time(DART) ionization source. Ionization was carried out in positive ionization mode. Mass spectrometer conditions were: nebulizer pressure, 35 psig; capillary voltage, 4000 V; drying gas flow, 12 L/min at 350°C; fragmentor voltage, 175 V.

CID: Tandem MS were performed using MS/MS acquisition function of Agilent MassHunter Acquisition interface. The analyte ions of interest were isolated using a narrow window (~1.3). The collision energy was 20 eV

The LC-Q-TOF was operated using an HP xw4600 Workstation computer. Data collection and analysis were performed respectively using Agilent MassHunter Acquisition and Agilent MassHunter Qualitative Analysis B.06.00. Calibration of the mass spectrometer was performed per manufacturer settings.

4.4.4 Microfluidic Extraction

Nanofibers were cut into 2mm diameter piece and then immersed into the diluted drug standards for 5 seconds for sample preparation. A set of experiment with different immersion time has been tested before. There is no significant difference between 5 seconds and 10min immersion. So 5 seconds immersion is selected to gain fast sample preparation rate.

HPLC grade methanol and acetonitrile were used as extraction solvent. Totally 4 solvent-fill-and-extract were set. No heating required, all extractions were done at room temperature.

4.4.5 HPLC separation

LC: Chromatogram was performed with an Agilent Poroshell^{TM} 120 EC – C18(2.7 µm, 3.0mm x 100 mm) reverse-phase column. The isocratic method used is 20% of mobile phase A and 80% of mobile phase B. The flow rate was 0.5 mL/min, the total run time was 16 minutes, and the equilibration time between samples was 1 minute. The injection volume of each sample was 1 µL.

DAD: Agilent Technologies 1260 liquid chromatograph is equipped with a photodiode array detector (DAD). The DAD was used on a 190 – 780 nm wavelength scan.

4.5 Results and discussion

4.5.1 Production of nanofibers

Polyacrylonitrile (PAN), polyvinyl alcohol (PVA) and polyvinylidene difluoride (PVDF) nanofibers have been prepared. After spinning, collected PVA nanofibers were then transferred to the oven to be heated under 150 °C for 2h, to achieve crosslinking, which is required for PVA nanofibers to improve its water stability. Figure 15 below is the Scanning Electron Microscope (SEM) photo of crosslinked PVA nanofibers.

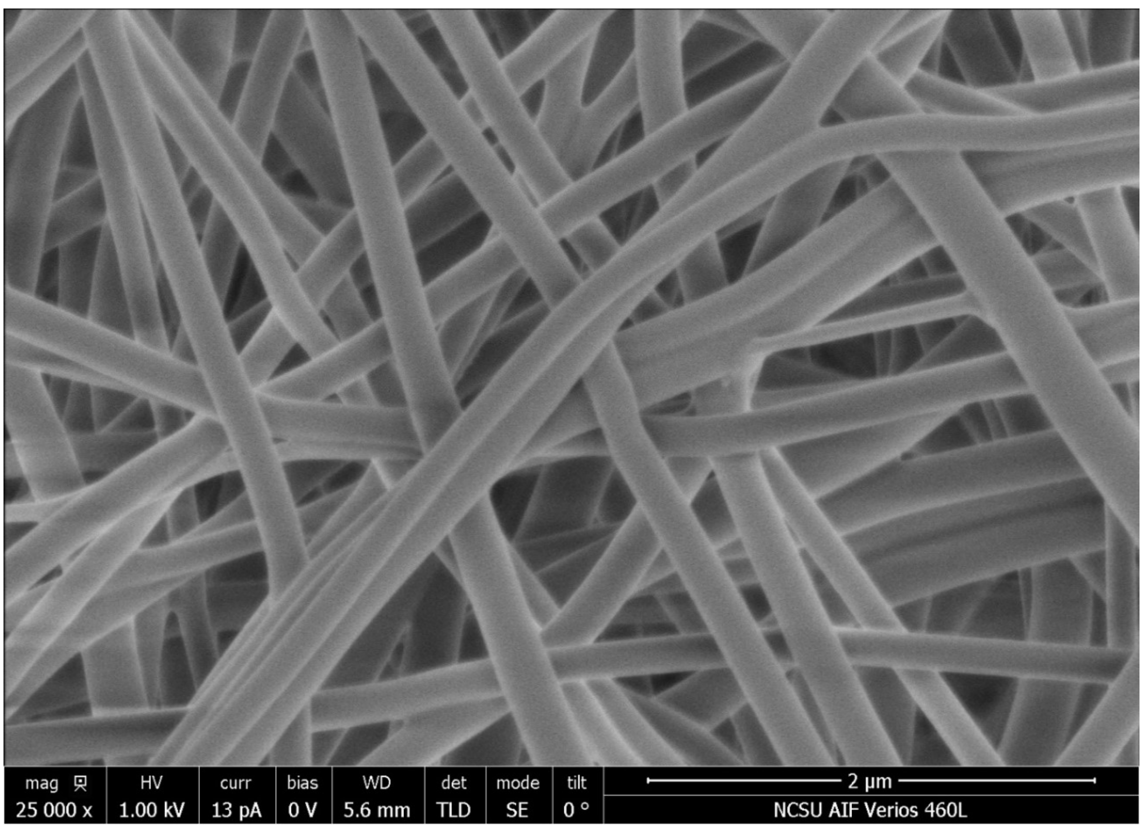

Figure 15 SEM graph of PVA nanofibers.

4.5.2 Microfluidic extraction and MS screening

The performance of the absorbance of PAN and PVDF nanofibers with respect to solutions containing the drugs of interest were compared with cotton fibers (control). Total Ion Current (TIC) signal was monitored on the mass spectrometer (all electronic conditions maintain the same) to compare all the fibers extraction by the microfluidic device. Figure 16 below shows a typical TIC of microfluidic extraction with 4 solvent fills.

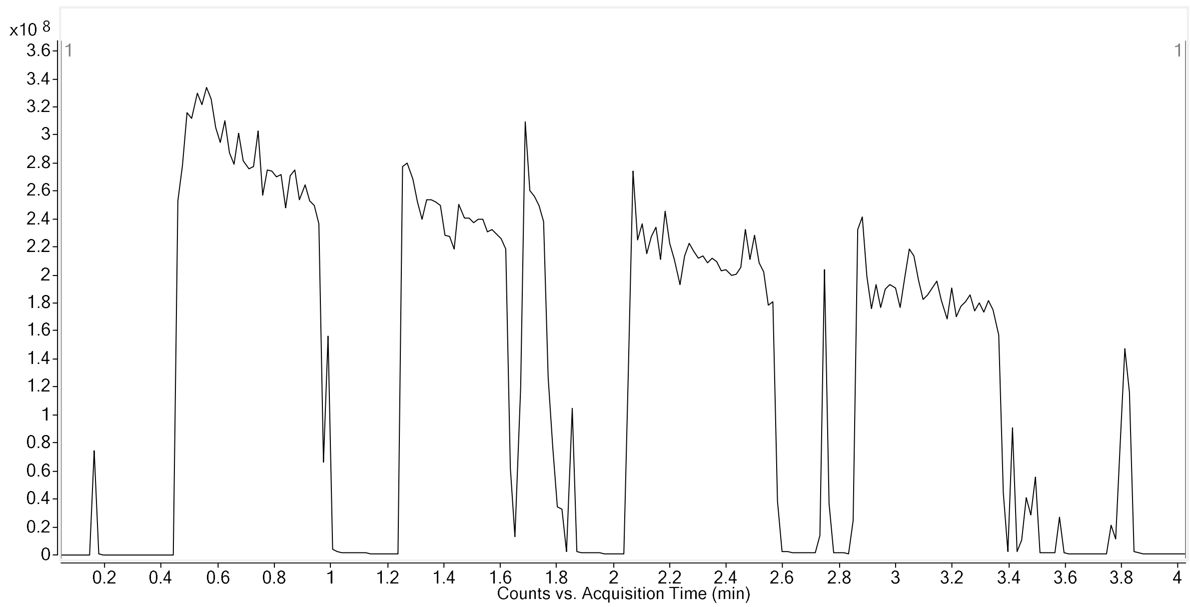

Figure 16 TIC of a microfluidic run with 4 buffer fills.

Spectra in Figure 16 is the comparison among nanofibers and cotton swab using MeOH as the extraction solvent. QTOF-MS results show that PAN has a greater potential to adsorb ibuprofen and Acetaminophen (APAP) samples compared to PVDF, which is reasonable due to its superior hydrophobicity which means fewer drug adsorption. In addition, PAN nanofiber demonstrated to absorb more ibuprofen and APAP compared to cotton fibers, since the signal from both drugs was not observed in the mass spectrometer from the cotton extraction. Comparing with PAN, cotton has lower capacity and poorer interaction with drugs, which leads to less drug attraction and storage, which leads to the absence of expected drug signals. Structure of ibuprofen and APAP are displayed in Figure 17.

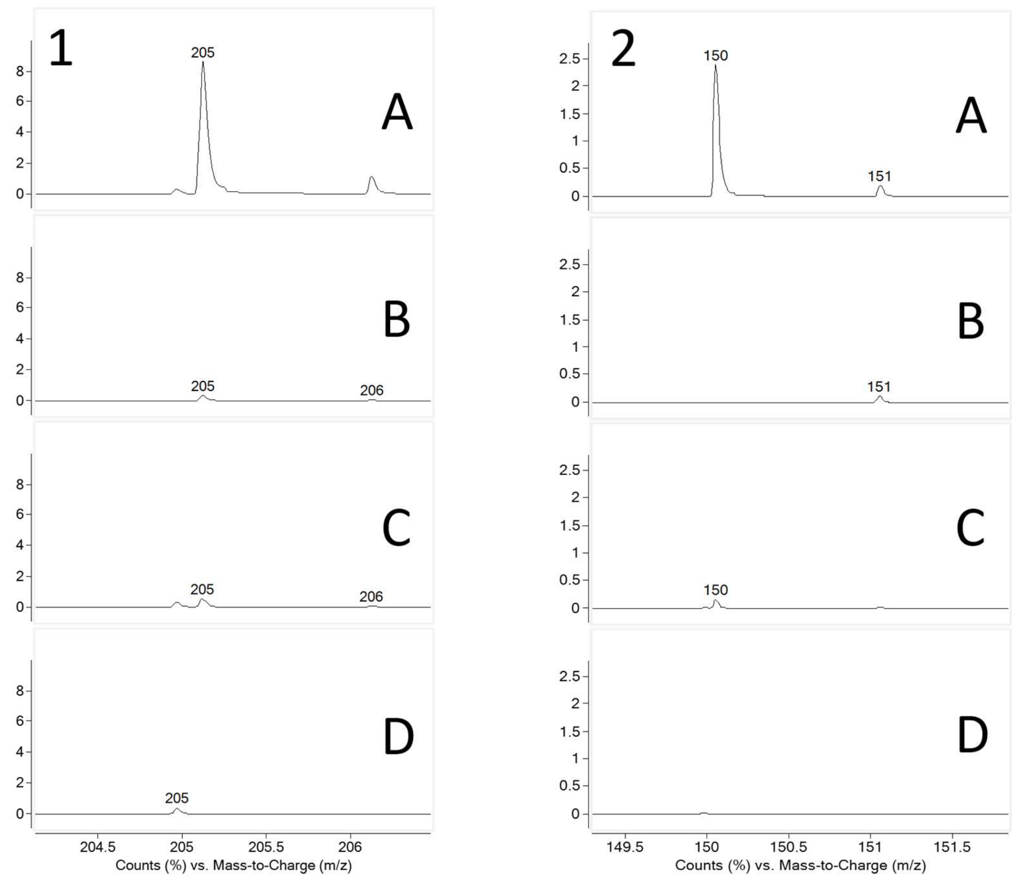

Figure 17 Comparison of nanofibers and a cotton swab. **A** is PAN, **B** is PVDF, **C** is cotton, **D** is blank.

Figure 17-1 is ibuprofen and Figure 17-2 is acetaminophen.

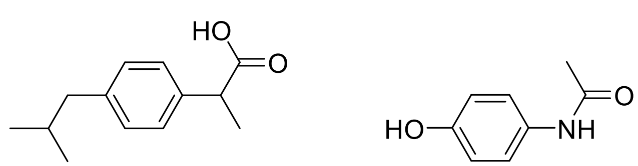

ibuprofen
Chemical Formula: $C_{13}H_{18}O_2$
Exact Mass: 206.1307

acetaminophen
Chemical Formula: $C_8H_9NO_2$
Exact Mass: 151.0633

Figure 18 Chemical structures and information of ibuprofen and acetaminophen.

Table 2 below shows the selectivity comparison among PVA, PAN, and direct injection. Experiments were replicated three times. Utilized drug standards were purchased from Cerilliant and then diluted to 100 ng/mL. Microfluidic extraction solvent was HPLC grade methanol. All the samples were run with Agilent 6520 Q-TOF mass spectrometry under the same electronic condition and experimental conditions. Comparing the nanofiber results to direct injection result could help eliminate the influence of ionization bias and thus helps focus on the selectivity. The difference between a nanofiber result and direct injection result indicates the difference of adsorption which is the selectivity. In diluted drug standard M-025, methamphetamine and cocaine present completely different relative abundance when using PVA nanofibers and PAN nanofibers. In diluted drug standard O-020, even both PVA and PAN have the common methadone as the most abundant signal, the relative abundance of the other four drugs are relatively higher when using PAN than using PVA. This behavior shows the influence of nanofibers' chemical structures. Figure 18 shows the structures of all drugs analyzed.

Table 2 Relativity abundance of drugs extracted by MeOH from PVA and PAN nanofibers.

Drug in the standard solution	**PVA**	**PAN**	**Direct Injection**
(±)-Methamphetamine	30%±5%	100%	100%
Cocaine	100%	68%±6%	71%±5%
Heroin	14%±3%	31%±5%	27%±4%
(±)-Methadone	100%	100%	100%
Codeine & Hydrocodone	29%±4%	41%±5%	31%±2%

Table 2 (continued).

Meperidine	55%±3%	57%±5%	53%±4%
Oxycodone	11%±3%	18%±3%	15%±4%

All values are relative abundance. Methamphetamine, cocaine, and heroin are mixed together, methadone, codeine, hydrocodone, meperidine and oxycodone are mixed together.

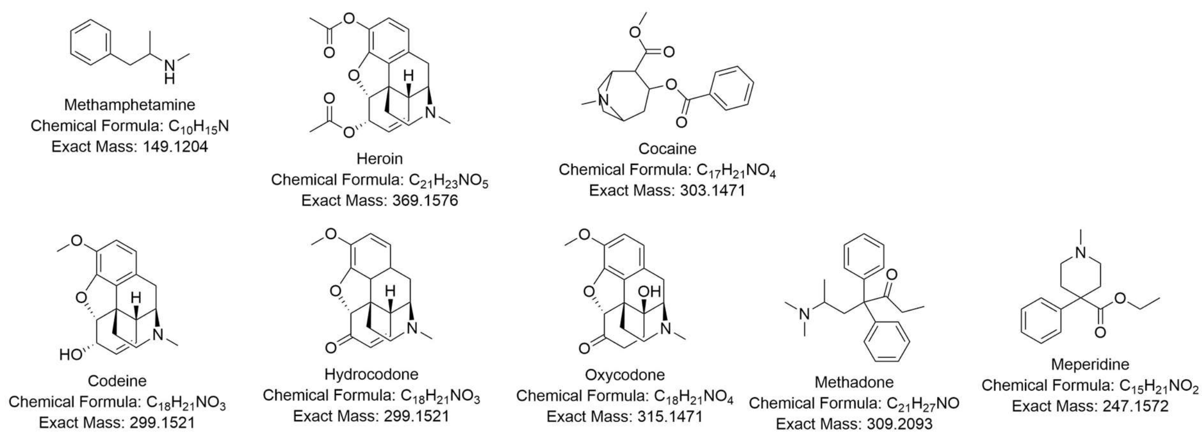

Figure 19 Chemical structures and information of all drugs in M-025 and O-020.

According to the structures, cocaine has five hydrogen-bonding acceptors and methamphetamine has only one acceptor. PVA has hydroxy functionalities that could act as hydrogen bonding donor, which PAN doesn't have. This difference may indicate the reason for the higher abundance of cocaine in PVA nanofibers. The stereostructure of heroin, codeine, hydrocodone, and oxycodone negatively affected the contact between the drug molecule and the nanofiber surface. The loose connection could explain why the number of hydrogen bonding acceptors doesn't provide a significant difference between PVA and PAN. In addition, the polarity of nanofibers and drugs will also affect the relative abundance.

Table 3 Relativity abundance of drugs extracted by ACN from PVA, PAN nanofibers, and direct injection.

Drug in the standard solution	PVA	PAN	Direct Injection
(±)-Methamphetamine*	19%±5%	78%±3%	70%±6%
Cocaine*	89%±3%	55%±3%	64%±3%
Heroine*	12%±5%	15%±4%	21%±4%
(±)-Methadone	100%	100%	100%
Codeine & Hydrocodone	23%±5%	31%±3%	27%±6%
Meperidine	31%±7%	40%±4%	37%±5%
Oxycodone	15%±4%	16%±3%	15%±5%

*Most abundant signal is 112.9857, which is trifluoroacetate, a component in tuning mix, acts as a background signal.

In order to understand the influence of the extraction solvent. Another experiment with the same drug standard solutions but different extraction solvent was performed. At this time, the utilized solvent was acetonitrile (ACN). Results are shown in Table 3 above. Comparing with MeOH, ACN has a lower polarity and based on its structure there ACN is only an H-bonding acceptor, hence reducing its ability to form hydrogen bonding with drug molecules. As expected, unlike the MeOH extraction result showed before in Table 2, almost all drugs' relative abundance decreased. When comparing to the direct injection result, the selectivity could still be observed but not as significant as MeOH extraction experiment. Since the amount of drug adsorption remains same if using same nanofibers, this decreased relative abundance means less drug was extracted. Otherwise, the drugs are still partially trapped inside the nanofibers after ACN extraction. This phenomenon shows that ACN is not a good extraction solvent comparing to MeOH because of its lower polarity and weak hydrogen bonding interaction with drugs.

4.5.3 Conclusion

Two types of nanofibers were successfully produced by electrospinning. They present selectivity on different drug structures based on the hydrogen bonding interaction and polarity. Stronger interaction will lead to more adsorption, and will even "trap" the drugs during extraction based on the choice of extraction solvent. The microfluidic extraction device provides four extractions in a single run within 3.5 min. This rapid extraction with minimal sample requirement and solvent consumption helps improve the efficiency for drug analysis. Q-TOF mass spectrometry provides accurate screening and identification based on exact mass measurement.

5. Study of drug selectivity based on the influence of intermolecular interactions between drugs and the functionalities of nanofibers

5.1 Abstract

The different organic group functionalities present on nanofibers are responsible for having different polarities and can affect the possibility to form hydrogen bonding. These characteristics will influence the intermolecular interaction between the drugs and the nanofibers and eventually, lead to a different selectivity. The elution profile has been measured to study and describe the influence of intermolecular interaction. A new chitosan nanofiber has been prepared to provide a nanofiber with mostly the ability to form hydrogen bonding. In addition, π-π stacking was

introduced by preparing new PVA nanofiber with graphene oxide composites. KNIME was used to quantitatively calculate the number of hydrogen bonding donor/acceptor and the XLogP, to provide a perspective understanding of the intermolecular interaction.

5.2 Introduction

In Chapter 4, MS analysis shows the difference of relative abundance of drugs when examining the same drug standard solution using different nanofibers. This result indicates the different selectivity based on the intermolecular interaction between the drugs and the functionalities of nanofibers. In addition, the polarity of solvent may also affect the drug extraction. Three key factors were proposed: 1. The ability to form hydrogen bonding between drugs and nanofibers, 2. The polarity of nanofibers, 3. The polarity of drugs. Both polarities affect the Van der Waals interaction between drugs and nanofibers.

To understand how the intermolecular interactions would influence the selectivity, the elution profile of microfluidic extraction has been measured. From the elution profile, it is easy to observe how the relative abundance changes during microfluidic extraction, which presents the retention of a specific drug on a specific nanofiber. Chitosan nanofiber has been prepared to promote more hydrogen bonding interactions. A new type of intermolecular interaction, π-π stacking has been introduced to PVA nanofibers by preparing PVA with graphene oxide composites.

Because of its excellent conductivity coming from the π system, graphene has been widely utilized in the preparation of high efficiency electronic devices.[93,95-97] The oxygen-rich groups on the graphene oxide could provide hydrogen bonding interaction sites, thus the stronger interactions between metallic ions and oxygen-rich groups extended the applications.[93,95,97]

To quantitatively describe the polarities of the drugs, XLogP[98] was introduced in this study. The partition coefficient abbreviated P, is defined as a particular ratio of the concentrations of a solute between the two solvents (a bi-phase of liquid phases), specifically for un-ionized solutes, and the logarithm of the ratio is thus LogP. When one of the solvents is water and the other is a non-polar solvent, then the LogP value is a measure of lipophilicity or hydrophobicity. The defined precedent is for the lipophilic and hydrophilic phase types to always be in the numerator and denominator. Normally, LogP means the partition coefficient of octanol and water in the pharmaceutical field to describe the hydrophilicity or lipophilicity of the drugs, which is corresponding to the polarity. The XLogP is a program for the prediction of the octanol/water partition coefficients of organic compounds. The XLogP was developed by the Institute of Physical Chemistry, of the Peking University and was first published in 1997. It is at least as accurate and more versatile as commercially available programs such as CLogP. It also has been tested by researchers in the Pharmaceutical Products Division of Abbott Laboratories for LogP prediction. XLogP is based on a group contribution method, but with some corrections (e.g. for the nature of the first neighbor of a group). The group contribution was developed using a training set of 1831 organic compounds.

In 2004, a team of software engineers at the University of Konstanz developed Konstanz Information Miner (KNIME), which is a free and open-source data analytics and mining platform. Compared with other data mining software such as SPSS and SAS, KNIME was famous because of its versatility and its friendly user interface. Traditional cheminformatics platforms rely on command line interfaces to operate, which considerably hinders their application as they require the operator to have certain training in command line language. KNIME, on the other hand, has a Graphic User Interface (GUI) and modular functionality, which greatly facilitates the operation as well as the modification of calculation as the operator could change the functionality of the whole workflow by connecting and disconnecting nodes. Datasets obtained from different sources could be integrated into one workflow. Currently, KNIME is usually used in biological as well as pharmaceutical applications.[99] The introduction of KNIME in this project promotes the combination of cheminformatics and forensic science. In this chapter, KNIME was used to calculate the number of hydrogen bonding donors and acceptors, and the XLogP which indicates the polarity of the drugs.

5.3 Materials

5.3.1 Solvent

HPLC grade acetonitrile and methanol were purchased from J.T.Baker, Deionized water was obtained from ELGA Purelab Ultra AN MK2. Porcine blood with heparin was obtained from NC State University, College of Veterinary Medicine.

5.3.2 Other supplies

Disposable Luer-slip plastic syringes (1 mL), Millex-GV 13 mm, 0.22 μm polyvinylidene fluoride (PVDF) filters, syringe needles (0.52 mm O.D. x 0.26 mm I.D., 25 gauge), and Fisherbrand 15 x 45 mm, 1-dram glass vials were purchased from Fisher Scientific. Amber screw top glass vials (2 mL) were purchased from Agilent Technologies (Part number: 5188-6535).

5.3.3 Drug Standards

Drug standards M-025, O-020, and S-038 were purchased from Cerilliant Inc.

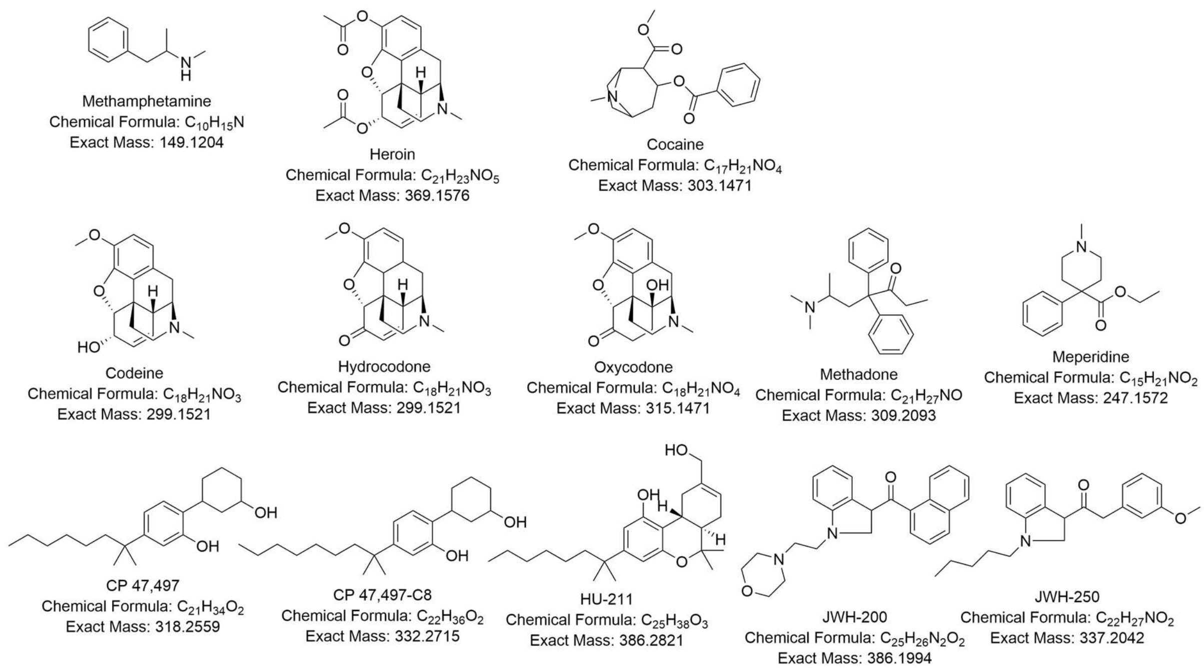

Figure 20 Chemical structures and information of all drugs in M-025, O-020, and S-038.

5.4 Experiments and instrumentation

5.4.1 Sample preparation

All drug standards were prepared for analysis by diluting in 1 mL of methanol or porcine plasma in a 1-dram Fisherbrand 15 x 45 mm, glass vial to make concentration 10 ppm. The diluted samples were transferred into 2-mL Agilent amber screw top glass LC vials (Part number: 5188-6535) for analysis. Porcine plasma was separated from porcine blood by using a centrifuge set at 2400 rpm for 10 min.

5.4.2 Nanofiber preparation by electrospinning

Polyacrylonitrile (PAN), polyvinyl alcohol(PVA) and chitosan nanofibers were prepared for this study. These nanofibers were selected due to their structure (functionality) and ease of control of the fiber diameter during production. The preparation of the PAN nanofibers by electrospinning was performed by making a solution of 2.4 g of polyacrylonitrile (PAN, Mw = 150,000, Sigma–Aldrich) and mixing it with 30 g of N,N-dimethylformamide, followed by mechanical stirring at 50 °C for 24 h. The solution was transferred to a syringe and was electrospun into nanofibers under a high voltage of 15 kV. During electrospinning, the needle-collector distance and the feed rate were fixed at 15 cm and 0.75 mL/min, respectively. For PVA nanofibers, For Chitosan nanofibers, preparation of a solution of acetic acid (90% aqueous) was mixed with chitosan (MW = 190,000, Sigma–Aldrich) to obtain a 5% wt. solution, which was stirred at 25°C for 12 h. The solution was transferred to a syringe and was electrospun into nanofibers under a high voltage of 16 kV. During electrospinning, the needle-collector distance and the feed rate were fixed at 10 cm and 0.4 mL/h, respectively. After preparation, PVA and Chitosan nanofibers were then transferred into the oven to be heated for 4 hours to get crosslinked. This process is necessary to avoid dissolution in water.

5.4.3 Mass Spectrometry

MS: The Agilent Technologies 1260 liquid chromatography is coupled to an Agilent Technologies 6520 Accurate-Mass Quadrupole–Time-of-Flight (Q-TOF) mass spectrometry equipped with an electrospray ionization (ESI) source or direct analysis in real time (DART) ionization source. Ionization was carried out in positive ionization mode. Mass spectrometer conditions were: nebulizer pressure, 35 psig; capillary voltage, 4000 V; drying gas flow, 12 L/min at 350°C; fragmentor voltage, 175 V.

CID: Tandem MS were performed using MS/MS acquisition function of Agilent MassHunter Acquisition interface. The analyte ions of interest were isolated using a narrow window (~1.3). The collision energy was 20 eV

The LC-Q-TOF was operated using an HP xw4600 Workstation computer. Data collection and analysis were performed respectively using Agilent MassHunter Acquisition and Agilent MassHunter Qualitative Analysis B.06.00. Calibration of the mass spectrometer was performed per manufacturer settings.

5.4.4 Microfluidic Extraction

Nanofibers were cut into 2mm diameter piece and then immersed into the diluted drug standards for 5 seconds for sample preparation. HPLC grade methanol was used as the extraction solvent. Totally 12 solvent-fill-and-extract were set. No heating required all extractions were done at room temperature.

5.5 Results and discussion

5.5.1 KNIME calculation

KNIME calculation results are shown in Table 4. First, three drugs are in standard M-025, then the following five drugs that are in standard O-020, the rest of the drugs are in standard S-038. Obviously, cocaine, heroin, hydrocodone, and JWH-200 has the highest number of hydrogen bonding acceptors. In addition, only 6 out of 13 drugs have hydrogen bonding donors, and all these 6 drugs have only 1 or 2 hydrogen bonding donors. It is also easy to see that all S-038 drugs have relatively higher XLogP than M-025 drugs and O-020 drugs, which means higher lipophilicity, or in another hand, lower polarity.

Table 4 Molecular information of all drugs calculated by KNIME.

Drug name	XLogP	H-Bond Acceptors	H-Bond Donors
Methamphetamine	2.152	1	1
Cocaine	2.307	5	0
Heroine	1.421	4	0
Meperidine	2.63	3	0
Methadone	4.592	2	0

Table 4 (continued).

Codeine	0.811	2	1
Hydrocodone	1.097	4	0
Oxycodone	0.012	3	1
CP 47, 497	6.965	1	2
CP 47, 497 C8	7.534	1	2
HU-211	7.405	1	2
JWH-200	4.057	4	0
JWH-250	6.438	2	0

5.5.2 Elution profile of three drug standard mixture with PVA nanofiber

Three figures in figure 18 demonstrate the elution profile of the three-drug standard mixtures with PVA nanofibers (the elution solvent is HPLC grade methanol).

In M-025, all three drugs have very rarely changed their relative abundances during 12 extractions. This means the intermolecular interaction between drugs and nanofiber functionalities are steady. As the conclusion in chapter 4, the highest relative abundance of cocaine indicates more adsorption by PVA nanofibers, which is the selectivity.

In O-020, methadone has the highest relative abundance during all 12 extractions. The meperidine, codeine, and hydrocodone have a gradual relative abundance change. Their increase-decrease elute profile indicates that more solvent extractions are needed to elute. These drugs are more sticky on the nanofibers comparing to methadone.

In S-038, all the relative abundance dramatically dropped after 6^{th} extraction. This quick drop means the drugs are barely sticky attached on the nanofibers and can be easily eluted. Otherwise, it indicates the weak intermolecular interaction between S-038 drugs and PVA nanofibers.

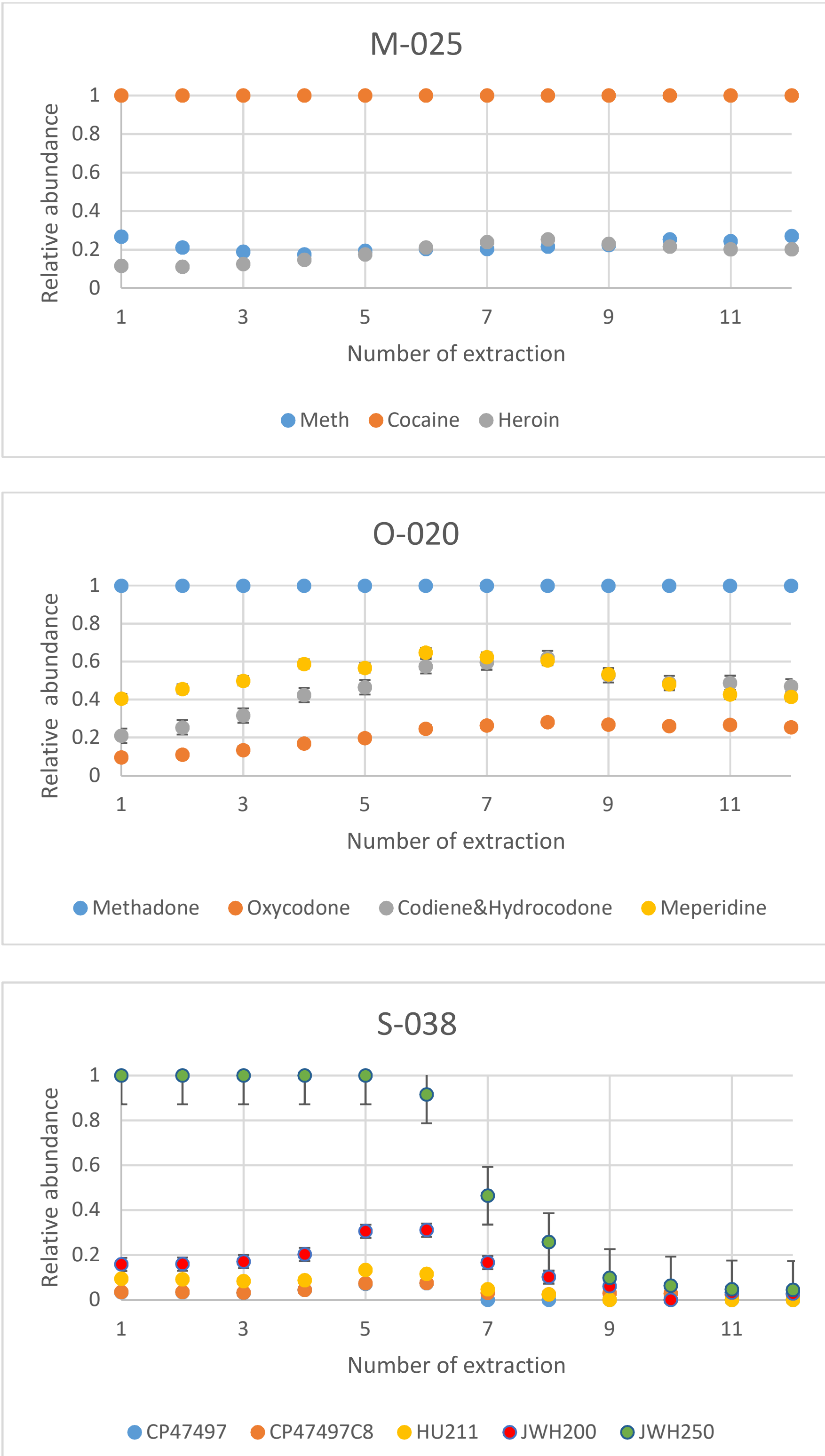

Figure 21 Elution profile of the three drug standard mixtures with PVA nanofibers.

5.5.3 Elution profile of three drug standard mixture with PAN nanofiber

Figure 18 shows the elution profile of the three drug standard mixtures with PAN nanofibers. The elution solvent is HPLC grade methanol. In M-025, unlike the PVA nanofibers, methamphetamine has the highest relative abundance at first, but it slowly dropped after 8^{th} extraction; at the meantime, the relative abundance of cocaine slightly increased and then dropped. Since methamphetamine and cocaine have similar XLogP values (2.152 vs 2.307), the affinity between methamphetamine and PAN nanofibers, and the affinity between cocaine and PVA nanofibers could be explained by the number of hydrogen bonding acceptors. As the result in Table 4, cocaine has five hydrogen-bonding acceptors and methamphetamine only have one. This indicates that cocaine has much higher chance to form hydrogen bonding with the hydroxy groups from PVA, this is the reason why cocaine dominated the spectra in PVA; in another hand, since PAN doesn't have any hydrogen bonding donors, only methamphetamine, which has one hydrogen bonding donor could form a hydrogen bonding with PAN. However, considering the weakness hydrogen bonding formation of nitrile group of PAN, only one hydrogen bonding is not strong enough to make a significant difference on relative abundance

In O-020, all drugs have a steady relative abundance with few changes. This indicates the strong and consistent intermolecular interaction between O-020 drugs and PAN nanofibers.

In S-038, JWH-250 presented the highest relative abundance at the beginning, but then dropped quickly. In addition, all the other four drugs demonstrated very low relative abundance during all 12 extractions. This all-decrease relative abundance shows the drugs are less sticky on the nanofibers, which indicates a weak interaction between drugs and PAN nanofibers.

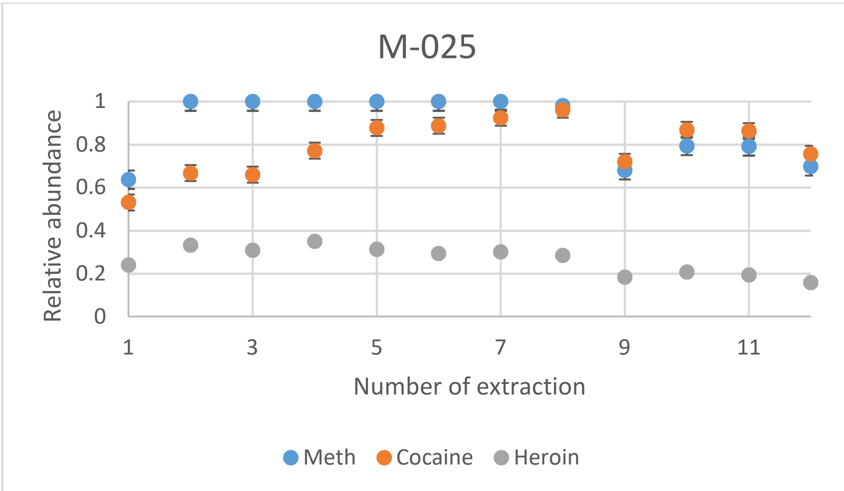

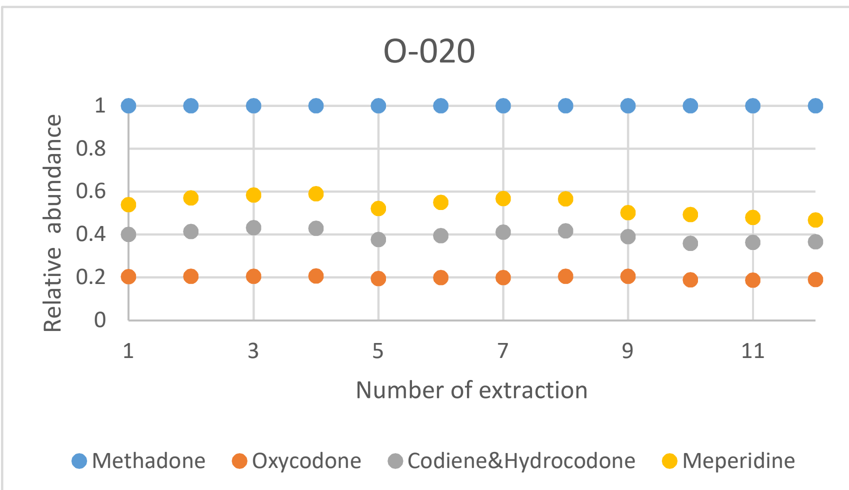

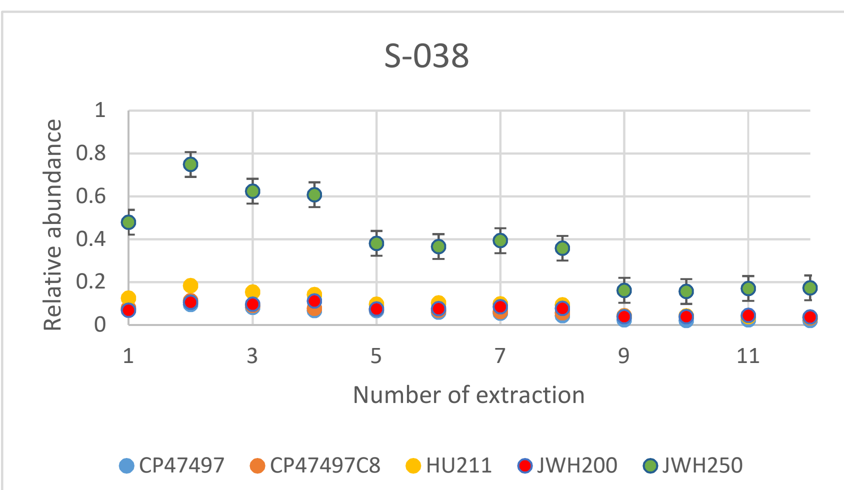

Figure 22 Elution profile of the three drug standard mixtures with PAN nanofibers.

5.5.4 Elution profile of 3 drug standard mixture with chitosan nanofiber

Figure 18 shows the elution profile of the three drug standard mixtures with chitosan nanofibers. The elution solvent is HPLC grade methanol. In this case, chitosan was selected because its high-hydrophilic structure with plentiful hydroxy and amino groups could help amplify the influence of hydrogen bonding formation.

In M-025 standard, all three drugs present very clear retention-elution peak, and cocaine always has the highest relative abundance among three drugs, just like the phenomenon in M-025 with PVA nanofibers. This indicates that hydrogen bonding is the key factor in this scenario.

In O-020 standard, methadone was highest at the beginning but dropped after 7th extraction. In the meantime, all the other four drugs show slight retention. This behavior is similar to the elution profile of O-020 with PVA. The drops of methadone may come from its higher XLogP, The slightly higher lipophilicity lead to weaker interaction with chitosan nanofibers.

In S-038, the elution profile shows similar behavior to the elution profile in S-038 with PVA. But at this time JWH-200 was higher than before at the beginning. The reason might be its relatively lower XLogP and the highest number of hydrogen bonding acceptors.

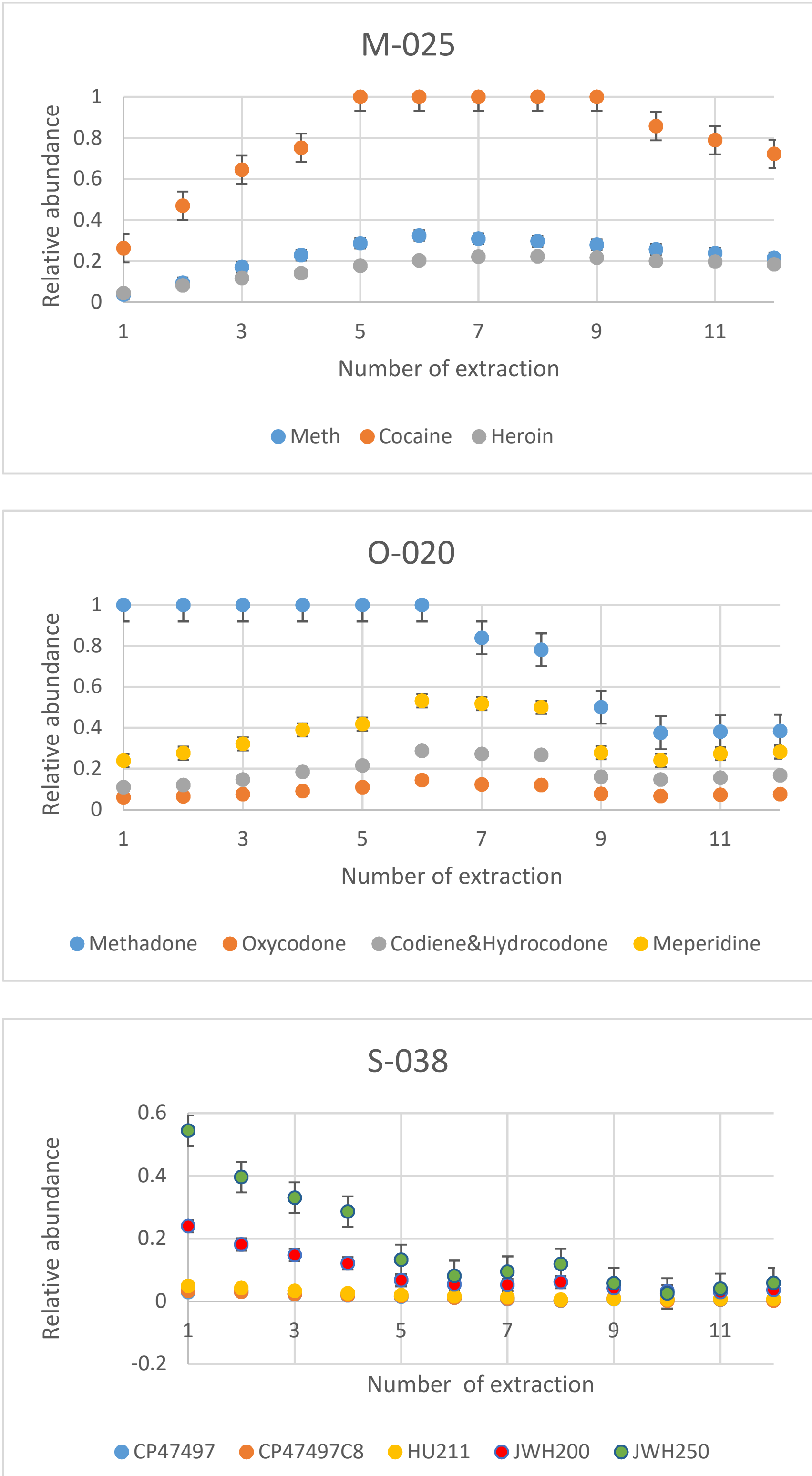

Figure 23 Elution profile of the three drug standard mixtures with Chitosan nanofibers.

5.5.5 Elution profile of three drug standard mixtures with PVA-GO nanofiber

Figure 18 shows the elution profile of the three drug standard mixtures with PVA-GO nanofibers. Elution solvent is HPLC grade methanol. The PVA composed with graphene oxide(GO) provides the same property of PVA plus more π-π stacking from GO. Comparing the figures below with figures of PVA helps to understand the influence of π-π stacking between drugs' aromatic πstructure with nanofibers.

In M-025, similar behavior was observed as M-025 with PVA. This means that hydrogen bonding is the key factor in this case. In O-020, the elution profile is completely different from O-020 with PVA. All drugs present increasing relative abundance, and the values became much higher at the 12^{th} extraction. This indicates that the extra π-π stacking in PVA helps trap the O-020 drugs, which leads to higher retention and finally higher relative abundance when eluted.

In S-038, even the relative abundances keep increasing all the time, but the values are relatively much lower than S-038 with PVA. This means there is barely pi-pi interaction between S-038 drugs with GO.

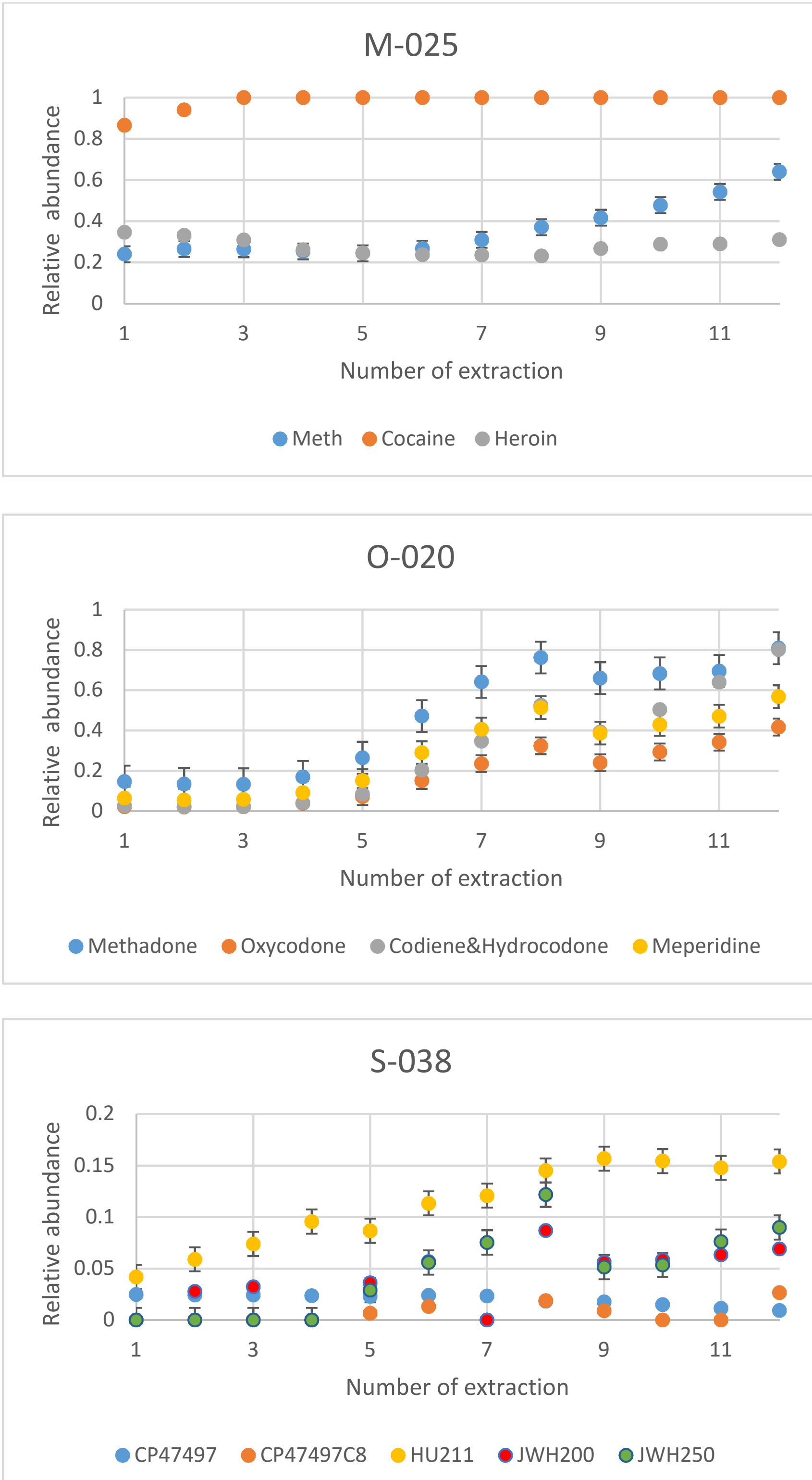

Figure 24 Elution profile of the three drug standard mixtures with PVA-GO nanofibers.

5.6 Conclusion

The elution profile could be used to describe how sticky the drug is on the nanofibers: A more sticky drug requires more extraction to reach a relatively high abundance. The KNIME software provided quantitatively description of molecular information of different drugs. From the XLogP values and number of hydrogen bonding acceptors and donors obtained from KNIME, the reason for each specific elution profile could be explained. By analyzing all the elution profiles, two key factors: Van der Waals interaction by polarity and hydrogen bonding between drugs and nanofibers could be confirmed. In addition, π-π stacking also affects the adsorption but only works on O-020 drugs. Thus, the proper nanofiber and drug couple could be preliminary selected based on KNIME calculation.

6. Screening of drugs in porcine plasma using nanofiber-MFD and method validation

6.1 Abstract

North Carolina faces an opioid crisis that has rapidly intensified in recent years. The screening of opioids became a major drug analysis work. In drug analysis, the analysis of a complex mixture is a costly and time-consuming work for researchers in forensic lab. When the mission of analysis of specific drug molecules in a normal forensic postmen-blood sample comes up, we are expecting to qualitatively and quantitatively finish this work with simple microfluidic-MS analysis without time-consuming sample pretreatment or LC separation. In previous chapters, the selectivity of drug screening using nanofibers has been discussed. In this chapter, the developed method will be evaluated and validated by following FDA quantitation standards.

6.2 Introduction

Like many other states, North Carolina faces an opioid crisis that has rapidly intensified in recent years. From 1999 to 2016 more than 12,000 North Carolinians died from opioid-related overdoses.[94] This epidemic is devastating families and communities. It is overwhelming medical providers and is straining prevention and treatment efforts. Addressing this epidemic requires interventions such as judicious prescribing of opioids, community-based prevention efforts, broader naloxone distribution, law enforcement efforts to curb drug trafficking, and harm reduction efforts like safe syringe programs.

The root causes of this epidemic are known. Many studies have shown that opioid overdose deaths at a population level are correlated with prescribing rates of opioids like hydrocodone and oxycodone[100-102]. Heavy marketing of these drugs to physicians and patients, in addition to a well-intentioned but flawed emphasis on the use of pain scales, led to an over-reliance on opioids. Those dynamics, coupled with the addictive potential of these drugs, have resulted in the epidemic of drug addiction and overdose gripping our state and our nation.

In the last several years, the problem has been compounded by cheap and easy access to heroin that often contains fentanyl or fentanyl analogs. These opioids are much more potent than prescription opioids and their availability and low cost compared to prescription drugs has led people to shift their consumption.

In this chapter, the drug standard opioid multi compound (O-020) and internal standards are selected to validate the developed quantitative drug analysis method to evaluate the performance of nanofibers on opioids testing. The porcine plasma solutions of O-020 are prepared to mimic the post-mortem plasma which would be a common sample in a forensic laboratory. This quantitation method was validated based on the U.S. Food and Drug Administration (FDA) biological quantitation standards.[103]

6.3 Materials

6.3.1 Solvent

HPLC grade acetonitrile and methanol were purchased from J.T.Baker, Deionized water was obtained from ELGA Purelab Ultra AN MK2.

Porcine blood with heparin was obtained from NC State University, College of Veterinary Medicine.

6.3.2 Other supplies

Disposable Luer-slip plastic syringes (1 mL), Millex-GV 13 mm, 0.22 μm polyvinylidene fluoride (PVDF) filters, syringe needles (0.52 mm O.D. x 0.26 mm I.D., 25 gauge), and Fisherbrand 15 x 45 mm, 1-dram glass vials were purchased from Fisher Scientific. Amber screw top glass vials (2 mL) were purchased from Agilent Technologies (Part number: 5188-6535).

6.3.3 Drug Standards

Drug standards O-020 and internal standards of meperidine, methadone, and oxycodone were purchased from Cerilliant Inc.

6.4 Experiments and instrumentation

6.4.1 Sample preparation

All drug standards were prepared for analysis by diluting in 1 mL of acetonitrile or methanol in a 1-dram Fisherbrand 15 x 45 mm, glass vial to make concentration 10 ppm. The diluted samples were transferred into 2-mL Agilent amber screw top glass LC vials (Part number: 5188-6535) for analysis.

Porcine plasma was separated from porcine blood by using a centrifuge set at 2400 rpm for

10 min.

6.4.2 Nanofiber preparation by electrospinning

Polyvinyl alcohol (PVA) nanofibers were prepared for this study. These nanofibers were selected due to its structure (functionality) and ease of control of the fiber diameter during production. The preparation of the PAN nanofibers by electrospinning was performed by making a solution of 2.4 g of polyacrylonitrile (PAN, Mw = 150,000, Sigma–Aldrich) and mixing it with 30 g of N,N-dimethylformamide, followed by mechanical stirring at 50 °C for 24 h. The solution was transferred to a syringe and was electrospun into nanofibers under a high voltage of 15 kV. During electrospinning, the needle-collector distance and the feed rate were fixed at 15 cm and 0.75 mL/min, respectively.

After preparation, PVA nanofibers were then transferred into the oven to be heated for 4 hours to get crosslinked. This process is necessary to avoid dissolution in water.

6.4.3 Mass Spectrometry

MS: The Agilent Technologies 1260 liquid chromatography is coupled to an Agilent Technologies 6520 Accurate-Mass Quadrupole–Time-of-Flight (Q-TOF) mass spectrometry equipped with an electrospray ionization (ESI) source or direct analysis in real time(DART) ionization source. Ionization was carried out in positive ionization mode. Mass spectrometer conditions were: nebulizer pressure, 35 psig; capillary voltage, 4000 V; drying gas flow, 12 L/min at 350°C; fragmentor voltage, 175 V.

CID: Tandem MS were performed using MS/MS acquisition function of Agilent MassHunter Acquisition interface. The analyte ions of interest were isolated using a narrow window (~1.3). The collision energy was 20 eV

The LC-Q-TOF was operated using an HP xw4600 Workstation computer. Data collection and analysis were performed respectively using Agilent MassHunter Acquisition and Agilent MassHunter Qualitative Analysis B.06.00. Calibration of the mass spectrometer was performed per manufacturer settings.

6.4.4 Microfluidic Extraction

HPLC grade methanol and acetonitrile were used as extraction solvent. Totally 4 solvent-fill-and-extract were set. No heating required all extractions were done at room temperature.

6.4.5 Preparation of calibration solution

A set of 6 O-020 drug standard with internal standards methadone-D4, meperidine-D3 and oxycodone-D3 solutions were prepared to make a calibration curve. One extra solution will be used to calculate precision. PVA nanofibers were utilized as drug adsorption substrate and were cut into a 2 mm round piece using puncher. Detail of calibration solutions shows below in table 5 below:

Table 5 Preparation of calibration solutions.

Drug / Conc. μg/mL.	Spiked Volume				
	O-020	**Methadone -D4**	**Meperidine -D3**	**Oxycodone -D3**	**Porcine plasma**
0.05	2μL	5μL	5μL	5μL	983μL
0.125	5μL	5μL	50μL	5μL	980μL
0.25*	**10μL**	**5μL**	**5μL**	**5μL**	**975μL**

Table 5 (continued).

0.375	15μL	5μL	5μL	5μL	970μL
0.5	20μL	5μL	5μL	5μL	965μL
0.75	30μL	5μL	5μL	5μL	955μL
1	40μL	5μL	5μL	5μL	945μL

*Bolded solution will be used as "unknown" to calculate precision

All calibrations were performed and replicated 6 times in 4 different days, 3 out of 6 were performed on the same day to obtain intra-day quantitation result. All-day results, inter-day result, and intra-day result will be compared and discussed in the following section.

6.5 Results and discussion

6.5.1 Linear regression result

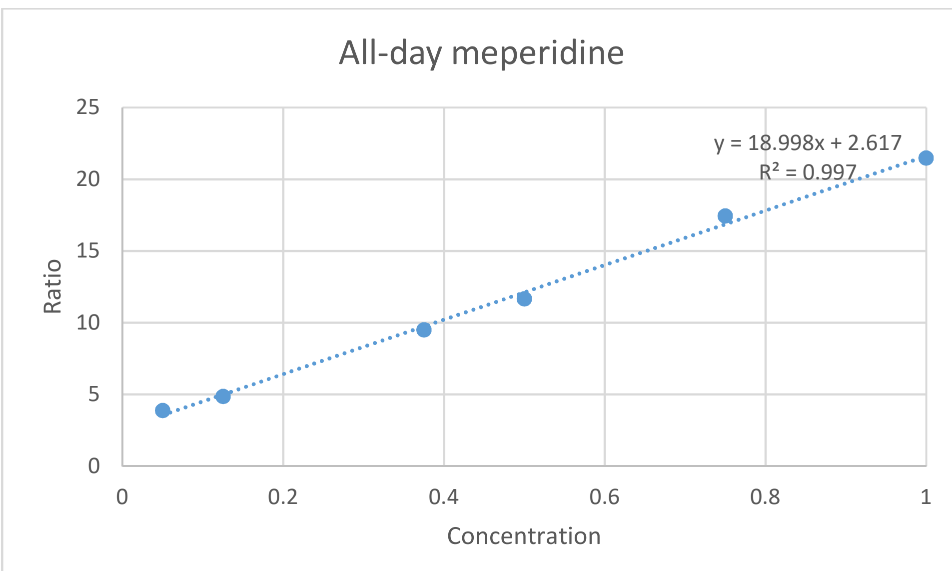

Figure 25 Linear fit figure of inter-day meperidine.

Figure 25 shows an example of a quantitation result. Here for the meperidine, R^2 is 0.997 which is outstanding for a QTOF mass spectrometer. The four tables below show the linear regression result of each drug. For oxycodone, its $[M+Na]^+$ ion was observed in the sample run with higher relative abundance, so the quantitation result based on $[M+Na]^+$ is also presented. The linear regression form is y = (X variable) x+ (Intercept Y), this formula will be used to calculate precision.

Table 6 Linear regression result of meperidine.

Meperidine	X variable	Intercept Y	R^2
All-day	19.00±3.11	2.62± 1.54	0.99±0.01
Inter-day	19.11±3.42	2.57±2.07	0.99±0.01
Intra-day	18.85±3.38	2.68±0.83	0.99±0.01

Table 7 Linear regression result of methadone.

Methadone	X variable	Intercept Y	R^2
All-day	25.67±5.22	3.01±2.03	0.99±0.01
Inter-day	26.55±5.69	2.70±2.79	0.99±0.01
Intra-day	24.49±5.42	3.43±0.53	0.98±0.01

Table 8 Linear regression result of oxycodone.

Oxycodone	X variable	Intercept Y	R^2
All-day	5.97±1.63	2.60±1.07	0.98±0.01
Inter-day	6.47±2.11	2.53±1.44	0.99±0.01
Intra-day	5.31±0.37	2.69±0.53	0.98±0.01

Table 9 Linear regression result of oxycodone-Na.

Oxycodone-Na	X variable	Intercept Y	R^2
All-day	14.81±3.72	3.53±2.02	0.98±0.01
Inter-day	15.09±4.46	3.58±2.72	0.99±0.01
Intra-day	14.43±3.35	3.46±1.08	0.98±0.01

The results from four tables above present high R^2 values(>0.98), for each drug quantitation. The difference among all-day, inter-day and intra-day quantitation is not significant.

6.5.2 Sensitivity evaluation

Sensitivity was evaluated according to the average lower limit-of-detection (LLOQ)

Table 10 LLOD result of all drugs(ng/mL).

LLOD	All	Inter-day	Intra-day
Meperidine	51±3	66±3	45±4
Methadone	59±3	60±4	72±2
Oxycodone	41±3	76±3	77±2
Oxycodone+Na	30±3	61±3	65±2

Table 11 LLOQ result of all drugs(ng/mL).

LLOQ	All	Inter-day	Intra-day
Meperidine	156±9	199±8	136±12
Methadone	178±10	182±11	219±7
Oxycodone	124±9	232±8	234±5
Oxycodone+Na	90±8	185±8	196±7

The calculated LLOD values for different drugs fall into the range recommended by North Carolina Office of the Chief Medicine Examiner(NCOCME). Values are shown below in table 13. Both LLOQ and LLOD of oxycodone-Na are slightly better than oxycodone. This is because of the higher intensity of oxycodone-Na adduct signal.

Table 12 NCOCME recommended toxic LLOD values of selected drugs(ng/mL).

Drug	LLOD
Meperidine	>1000
Methadone	60~3100
Oxycodone	120~140

6.5.3 Accuracy evaluation

Accuracy was evaluated by comparing experimental abundances of each standard to theoretical values on one day (intra-day) and across three days (inter-day). Note that the concentration below calculated LLOD was eliminated. The intra-day and inter-day accuracy of the experimental abundances were well within the acceptable ±15% as shown in Table 13-16 below:

Table 13 Accuracy of Meperidine.

Meperidine	Inter-day Accuracy	Intra-day Accuracy
0.125	-3%±8%	-7%±10%
0.375	-2%±3%	-1%±8%
0.5	-4%±10%	-1%±7%
0.75	5%±1%	3%±7%
1	-1%±3%	-1%±5%

Table 14 Accuracy of Methadone.

Methadone	Inter-day Accuracy	Intra-day Accuracy
0.125	-9%±4%	-3%±3%
0.375	0%±7%	1%±3%
0.5	2%±8%	4%±12%
0.75	4%±3%	3%±4%
1	-3%±2%	-3%±5%

Table 15 Accuracy of Oxycodone.

Oxycodone	Inter-day Accuracy	Intra-day Accuracy
0.125	0%±6%	1%±9%
0.375	-5%±5%	3%±6%
0.5	5%±5%	3%±6%
0.75	-3%±3%	1%±5%
1	1%±2%	-2%±2%

Table 16 Accuracy of Oxycodone-Na.

Oxycodone-Na	Inter-day Accuracy	Intra-day Accuracy
0.125	-1%±3%	-2%±6%
0.375	-7%±2%	6%±7%
0.5	1%±5%	2%±3%
0.75	0%±4%	-3%±9%
1	1%±3%	0%±4%

A quantifying quality control standards of known concentration (250 ng/mL) was also been tested, and results are shown in the table below. All within ±15%.

Table 17 Accuracy of Oxycodone-Na.

Drug in 250ng/mL	Inter-day Accuracy	Intra-day Accuracy
Meperidine	-7%±3&	3%±5%
Methadone	-10%±4%	0%±8%
Oxycodone	-2%±3%	4%±7%
Oxycodone-Na	2%±6%	14%±2%

6.5.4 Precision evaluation

Precision was evaluated according to intra- and inter-day coefficients of variation (CV%), results are shown in the four tables below. All values are within the acceptable ±15%.

Table 18 Precision of Meperidine.

Meperidine	Inter-day Precision	Intra-day Precision
0.125	11%±2%	10%±2%
0.375	12%±7%	12%±4%
0.5	14%±10%	9%±5%
0.75	7%±5%	8%±6%
1	3%±3%	6%±6%

Table 19 Precision of Methadone.

Methadone	Inter-day Precision	Intra-day Precision
0.125	**7%**±1%	9%±1%
0.375	8%±3%	5%±2%
0.5	10%±5%	15%±8%
0.75	5%±4%	5%±4%
1	3%±3%	6%±6%

Table 20 Precision of Oxycodone.

Oxycodone	Inter-day Precision	Intra-day Precision
0.125	12%±3%	14%±6%
0.375	12%±4%	13%±5%
0.5	10%±5%	10%±6%
0.75	3%±2%	8%±6%
1	3%±3%	4%±4%

Table 21 Precision of Oxycodone-Na.

Oxycodone-Na	Inter-day Precision	Intra-day Precision
0.125	12%±2%	14%±3%
0.375	6%±2%	10%±4%
0.5	5%±3%	5%±3%
0.75	6%±5%	13%±9%
1	4%±4%	5%±5%

6.6 Conclusion

A drug screening method using nanofiber-Micro Fluidic Device-Mass Spectrometry has been developed. Reliable quantitative analysis was achieved using ESI-QTOF with internal standard. The method helps significantly reduce the time consumption by simplifying the sample preparation. Application on porcine plasma sample presents the great potential of this method on post mortem plasma drug analysis. This method has been evaluated validated. LLOD and LLOQ of plasma samples are qualifying the NCOCME recommendation. Accuracy and precision are acceptable according to FDA standards. [103]

7. Conclusion and Recommendation of future work

As a conclusion, a rapid, qualitative and quantitative analysis of drugs is possible using common and cost-effective instruments which involves a microfluidic extraction device and the quadrupole-time-of-flight (QTOF) mass spectrometry. In addition, the utilization of specific nanofibers provides selectivity on certain drugs based on the different intermolecular interactions. The intermolecular interactions between nanofibers and drugs are contributed by three key factors: the ability to form hydrogen bonds, the polarity of nanofibers and the polarity of drug molecules. My research shows that the more hydrogen bonds between nanofibers and drugs could enhance the drug adsorption and even made the adsorption more sticky, which means the drugs with strong interactions would have an increased relative abundance comparing to the direct injection, and may need more times of extraction to elute. This method has been applied on porcine plasma drug solution to mimic the common evidence, postmortem blood and its plasma, in forensic labs. The result shows three drugs in drug standard O-020 could be successfully quantified, and the quantitation falls into the NCOCME recommended range for toxic levels of drugs in blood. The method has also been successfully validated and evaluated and the accuracy and precision are acceptable according to FDA standards. [103]

Previous study demonstrated the potential of selective drug adsorption of certain nanofibers and its application using MFD-MS and three key factors have been addressed. The validation and evaluation confirmed that this method is reliable, as well as cost-effective and fast.

However, the detailed principle of the correlation between specific structure and the selectivity is not completely revealed since only polarity, hydrogen bonding and π-π stacking were discussed. Thus, in the future, different type of nanofibers and drugs should be chosen to continue this study on more interactions. The influence of molecular shape, size should be considered. More computing methods should also be involved to quantitatively describe the molecular properties and their effects.

From material science side, the parameters of nanofibers also play an important role. Obviously, the porosity and the diameter of fibers will significantly affect the adsorption. An expert in material science is highly welcomed to join this project and provide perspective view from other side.

REFERENCES

1. Teo WE, Ramakrishna S. A review on electrospinning design and nanofibre assemblies. *Nanotechnology*. 2006;17(14):R106.

2. Greiner A, Wendorff JH. Electrospinning: A fascinating method for the preparation of ultrathin fibers. *Angewandte Chemie International Edition*. 2007;46(30):5670-5703.

3. Brandt SD, King LA, Evans-Brown M. The new drug phenomenon. *Drug testing and analysis*. 2014;6(7-8):587-597.

4. Lledo-Fernandez C, Banks CE. An overview of quantifying and screening drugs of abuse in biological samples: Past and present. *Analytical Methods*. 2011;3(6):1227-1245.

5. Riviello RJ. *Manual of forensic emergency medicine: A guide for clinicians.* Jones & Bartlett Publishers; 2009.

6. Kintz P, Brunet B, Muller J, et al. Evaluation of the cozart DDSV test for cannabis in oral fluid. *Ther Drug Monit*. 2009;31(1):131-134.

7. Miyaguchi H, Takahashi H, Ohashi T, et al. Rapid analysis of methamphetamine in hair by micropulverized extraction and microchip-based competitive ELISA. *Forensic Sci Int*. 2009;184(1):1-5.

8. Bayne S, Carlin M. *Forensic applications of high performance liquid chromatography.* CRC Press; 2010.

9. Stacey RB, Unit T. Report on the erroneous fingerprint individualization in the madrid train bombing case. *historian*. 2005;404:294-2647.

10. World Health Organization. World drug report. *New York: United Nations Offices on Drugs and Crime (UNODC)*. 2012.

11. SWGDRUG. Scientific working group for the analysis of seized drugs (SWGDRUG) recommendations. . 2010.

12. Hedenus M. Eugen goldstein and his laboratory work at berlin observatory. *Astronomische Nachrichten*. 2002;323(6):567-569.

13. Kragh H. *Quantum generations: A history of physics in the twentieth century.* Princeton University Press; 2002.

14. Thomson JJ. LXXXIII. rays of positive electricity. *The London, Edinburgh, and Dublin Philosophical Magazine and Journal of Science*. 1910;20(118):752-767.

15. Griffiths J. A brief history of mass spectrometry. *Anal Chem*. 2008;80(15):5678-5683.

16. Dass C. *Fundamentals of contemporary mass spectrometry.* Vol 16. John Wiley & Sons; 2007.

17. Hu Q, Noll RJ, Li H, Makarov A, Hardman M, Graham Cooks R. The orbitrap: A new mass spectrometer. *Journal of mass spectrometry*. 2005;40(4):430-443.

18. Baldwin MA, McLafferty FW. Liquid chromatography-mass spectrometry interface-I: The direct introduction of liquid solutions into a chemical ionization mass spectrometer. *Org Mass*

Spectrom. 1973;7(9):1111-1112. http://onlinelibrary.wiley.com/doi/10.1002/oms.1210070913/abstract. doi: 10.1002/oms.1210070913.

19. Gross JH, SpringerLink (Online service). *Mass spectrometry: A textbook.* Berlin, Heidelberg: Springer Berlin Heidelberg; 2011. http://ncsu.summon.serialssolutions.com/2.0.0/link/0/eLvHCXMwbV07T8MwED5RGGArlIcJlTKyRI0Tp4knhoiKhQV1t2rHrSpVAaEg8fO5s5M0LZUiRc4pfuRxT993AOFcF8Vap3OULgRdkqCKoe2aG5ObOK7EkSMHujCM27dB1QKGG9hnDjTQIUUMABLdnvgucOn4eVtr6mWzRy3ojaQ0QiUb-U1OwYQRjIqUajyU8qN3xsQCfzNJOID4haLUdLkNzsynk7sz2zc4zz10T09MDtqcauy2aUvI6WkpBGhS7_5FW50QW4zhwlJmwzWc2foGLsuu1NsExu-oQodUir4h9AK8dgvB4nVZvkXUrWp9PCqh8CbqYnc43GdtHyAsVpURRhNwUSW4zaTlZCrIlaxMmsWCwb2fofrysBYKDTNBaGMMgiNK89sMqJNTIzNguEClt3q3bbG2FUexKJCJMHjult13efBeOI8ylaPlmDye7j2AK-_LpeMJzpvvHzv1T_YP57yoXA. 10.1007/978-3-642-10711-5.

20. Dawson PH. *Quadrupole mass spectrometry and its applications.* Elsevier; 2013.

21. Chernushevich IV, Loboda AV, Thomson BA. An introduction to quadrupole–time-of-flight mass spectrometry. *Journal of Mass Spectrometry*. 2001;36(8):849-865.

22. Stephens WE. A pulsed mass spectrometer with time dispersion. . 1946;69(11-1):691.

23. Cotter RJ. Time-of-flight mass spectrometry for the structural analysis of biological molecules. *Anal Chem*. 1992;64(21):1039A.

24. Mamyrin BA. Laser assisted reflectron time-of-flight mass spectrometry. *International Journal of Mass Spectrometry and Ion Processes*. 1994;131:1-19.

25. Cotter RJ. *Time-of-flight mass spectrometry: Instrumentation and applications in biological research.* Amer Chemical Society; 1997.

26. Guilhaus M. Principles and instrumentation in time-of-flight mass spectrometry. *J Mass Spectrom*. 1995;30(11):1519-1532.

27. Ioanoviciu D. Ion-Optical solutions in time-of-flight mass spectrometry. *Rapid communications in mass spectrometry*. 1995;9(11):985-997.

28. Mamyrin BA. Time-of-flight mass spectrometry (concepts, achievements, and prospects). *International Journal of Mass Spectrometry*. 2001;206(3):251-266.

29. Fuerstenau SD, Benner WH. Molecular weight determination of megadalton DNA electrospray ions using charge detection time-of-flight mass spectrometry. *Rapid Communications in Mass Spectrometry*. 1995;9(15):1528-1538.

30. Vestal ML. Modern MALDI time-of-flight mass spectrometry. *Journal of mass spectrometry*. 2009;44(3):303-317.

31. Yost RA, Enke CG. Selected ion fragmentation with a tandem quadrupole mass spectrometer. *J Am Chem Soc*. 1978;100(7):2274-2275.

32. Hopfgartner G, Varesio E, Tschäppät V, Grivet C, Bourgogne E, Leuthold LA. Triple quadrupole linear ion trap mass spectrometer for the analysis of small molecules and macromolecules. *Journal of Mass Spectrometry*. 2004;39(8):845-855.

33. Zhang N, Yang A, Rogers JD, Zhao JJ. Quantitative analysis of simvastatin and its β-hydroxy acid in human plasma using automated liquid–liquid extraction based on 96-well plate format and liquid chromatography-tandem mass spectrometry. *J Pharm Biomed Anal*. 2004;34(1):175-187.

34. Barbarin N, Mawhinney DB, Black R, Henion J. High-throughput selected reaction monitoring liquid chromatography–mass spectrometry determination of methylphenidate and its major metabolite, ritalinic acid, in rat plasma employing monolithic columns. *Journal of Chromatography B*. 2003;783(1):73-83.

35. Shushan B. A review of clinical diagnostic applications of liquid chromatography–tandem mass spectrometry. *Mass Spectrom Rev*. 2010;29(6):930-944.

36. Pistos C, Koutsopoulou M, Panderi I. A validated liquid chromatographic tandem mass spectrometric method for the determination of mirtazapine and demethylmirtazapine in human plasma: Application to a pharmacokinetic study. *Anal Chim Acta*. 2004;514(1):15-26.

37. Hara H, Uchimura T, Akashi N, et al. Simultaneous analytical method for the determination of TCH346 and its four metabolites in human plasma by liquid chromatography/tandem mass spectrometry. *Rapid communications in mass spectrometry*. 2004;18(4):377-384.

38. Whalen K, Gobey J, Janiszewski J. A centralized approach to tandem mass spectrometry method development for high-throughput ADME screening. *Rapid Communications in Mass Spectrometry: An International Journal Devoted to the Rapid Dissemination of Up-to-the-Minute Research in Mass Spectrometry*. 2006;20(10):1497-1503.

39. Higton DM. A rapid, automated approach to optimisation of multiple reaction monitoring conditions for quantitative bioanalytical mass spectrometry. *Rapid Communications in Mass Spectrometry*. 2001;15(20):1922-1930.

40. Whalen KM, Rogers KJ, Cole MJ, Janiszewski JS. AutoScan: An automated workstation for rapid determination of mass and tandem mass spectrometry conditions for quantitative bioanalytical mass spectrometry. *Rapid Communications in Mass Spectrometry*. 2000;14(21):2074-2079.

41. Coles R, Kushnir MM, Nelson GJ, McMillin GA, Urry FM. Simultaneous determination of codeine, morphine, hydrocodone, hydromorphone, oxycodone, and 6-acetylmorphine in urine, serum, plasma, whole blood, and meconium by LC-MS-MS. *J Anal Toxicol*. 2007;31(1):1-14.

42. Kaufmann A, Butcher P, Maden K, Walker S, Widmer M. Quantitative and confirmative performance of liquid chromatography coupled to high-resolution mass spectrometry compared to tandem mass spectrometry. *Rapid Communications in Mass Spectrometry*. 2011;25(7):979-992.

43. Majumdar TK, Vedananda S, Tse FL. Rapid analysis of MMI270B, an inhibitor of matrix metalloproteases in human plasma by liquid chromatography–tandem mass spectrometry: Matrix interference in patient samples. *Biomedical Chromatography*. 2004;18(2):77-85.

44. Matuszewski BK, Chavez-Eng CM, Constanzer ML. Development of high-performance liquid chromatography–tandem mass spectrometric methods for the determination of a new oxytocin receptor antagonist (L-368,899) extracted from human plasma and urine: A case of lack of specificity due to the presence of metabolites. *Journal of Chromatography B: Biomedical Sciences and Applications*. 1998;716(1-2):195-208.

45. Lu W, Clasquin MF, Melamud E, Amador-Noguez D, Caudy AA, Rabinowitz JD. Metabolomic analysis via reversed-phase ion-pairing liquid chromatography coupled to a stand alone orbitrap mass spectrometer. *Anal Chem*. 2010;82(8):3212-3221.

46. Douglas DJ, French JB. Collisional focusing effects in radio frequency quadrupoles. *J Am Soc Mass Spectrom*. 1992;3(4):398-408.

47. Krutchinsky AN, Chernushevich IV, Spicer VL, Ens W, Standing KG. Collisional damping interface for an electrospray ionization time-of-flight mass spectrometer. *J Am Soc Mass Spectrom*. 1998;9(6):569-579.

48. Watson JT, Sparkman OD. *Introduction to mass spectrometry: Instrumentation, applications, and strategies for data interpretation.* John Wiley & Sons; 2007.

49. Fernández de La Mora, Juan. The fluid dynamics of taylor cones. *Annu.Rev.Fluid Mech.* 2007;39:217-243.

50. Taylor GI, McEwan AD. The stability of a horizontal fluid interface in a vertical electric field. *J Fluid Mech*. 1965;22(01):1-15.

51. Cloupeau M, Prunet-Foch B. Electrohydrodynamic spraying functioning modes: A critical review. *J Aerosol Sci*. 1994;25(6):1021-1036.

52. Rayleigh L. XX. on the equilibrium of liquid conducting masses charged with electricity. *The London, Edinburgh, and Dublin Philosophical Magazine and Journal of Science*. 1882;14(87):184-186.

53. Gomez A, Tang K. Charge and fission of droplets in electrostatic sprays. *Physics of Fluids (1994-present)*. 1994;6(1):404-414.

54. Smith JN, Flagan RC, Beauchamp JL. Droplet evaporation and discharge dynamics in electrospray ionization. *The Journal of Physical Chemistry A*. 2002;106(42):9957-9967.

55. Grimm RL, Beauchamp JL. Evaporation and discharge dynamics of highly charged droplets of heptane, octane, and p-xylene generated by electrospray ionization. *Anal Chem*. 2002;74(24):6291-6297.

56. Kebarle P, Verkerk UH. Electrospray: From ions in solution to ions in the gas phase, what we know now. *Mass Spectrom Rev*. 2009;28(6):898-917.

57. Dole M, Mack LL, Hines RL, Mobley RC, Ferguson LD, Alice Md. Molecular beams of macroions. *J Chem Phys*. 1968;49(5):2240-2249.

58. Iribarne JV, Thomson BA. On the evaporation of small ions from charged droplets. *J Chem Phys*. 1976;64(6):2287-2294.

59. Znamenskiy V, Marginean I, Vertes A. Solvated ion evaporation from charged water nanodroplets. *The Journal of Physical Chemistry A*. 2003;107(38):7406-7412.

60. Cody RB, Laramee JA, Durst HD. Versatile new ion source for the analysis of materials in open air under ambient conditions. *Anal Chem*. 2005;77(8):2297-2302.

61. Cody RB. Review of direct analysis in real time (DART™) mass spectrometry. *Spectroscopy Europe*. 2006;18:S12.

62. Fernández FM, Cody RB, Green MD, et al. Characterization of solid counterfeit drug samples by desorption electrospray ionization and direct-analysis-in-real-time coupled to time-of-flight mass spectrometry. *ChemMedChem*. 2006;1(7):702-705.

63. Chernetsova ES, Bochkov PO, Ovcharov MV, Zhokhov SS, Abramovich RA. DART mass spectrometry: A fast screening of solid pharmaceuticals for the presence of an active ingredient, as an alternative for IR spectroscopy. *Drug testing and analysis*. 2010;2(6):292-294.

64. Chernetsova ES, Abramovich RA, Revel'skii IA. DART mass spectrometry: Rapid analysis of soft medicinal formulations. *Pharmaceutical Chemistry Journal*. 2012;45(11):698-700.

65. Carroll DI, Dzidic I, Stillwell RN, Haegele KD, Horning EC. Atmospheric pressure ionization mass spectrometry. corona discharge ion source for use in a liquid chromatograph-mass spectrometer-computer analytical system. *Anal Chem*. 1975;47(14):2369-2373.

66. Dzidic I, Carroll DI, Stillwell RN, Horning EC. Comparison of positive ions formed in nickel-63 and corona discharge ion sources using nitrogen, argon, isobutane, ammonia and

nitric oxide as reagents in atmospheric pressure ionization mass spectrometry. *Anal Chem*. 1976;48(12):1763-1768.

67. Robb DB, Covey TR, Bruins AP. Atmospheric pressure photoionization: An ionization method for liquid chromatography− mass spectrometry. *Anal Chem*. 2000;72(15):3653-3659.

68. Robb DB, Covey TR, Bruins AP. Atmospheric pressure photoionization (APPI): A new ionization technique for LC/MS. *Adv.Mass Spectrom*. 2001;15:391-392.

69. Tswett M. Physikalisch-chemische studien über das chlorophyll. die adsorptionen. *Berichte der Deutschen botanischen Gesellschaft*. 1906;24(316-323):20.

70. Lough WJ, Wainer IW. *High performance liquid chromatography: Fundamental principles and practice.* CRC Press; 1995.

71. Neue UD. *HPLC columns: Theory, technology, and practice.* Wiley-VcH; 1997.

72. Al-Hetlani E. Forensic drug analysis and microfluidics. *Electrophoresis*. 2013;34(9-10):1262-1272.

73. Verpoorte E. Microfluidic chips for clinical and forensic analysis. *Electrophoresis*. 2002;23(5):677-712.

74. Horsman KM, Bienvenue JM, Blasier KR, Landers JP. Forensic DNA analysis on microfluidic devices: A review. *J Forensic Sci*. 2007;52(4):784-799.

75. Piccin E, Dossi N, Cagan A, Carrilho E, Wang J. Rapid and sensitive measurements of nitrate ester explosives using microchip electrophoresis with electrochemical detection. *Analyst*. 2009;134(3):528-532.

76. Wang J, Pumera M, Chatrathi MP, et al. Single-channel microchip for fast screening and detailed identification of nitroaromatic explosives or organophosphate nerve agents. *Anal Chem*. 2002;74(5):1187-1191.

77. Liu Y, He J, Zhang R, Shi J, Abliz Z. Study of the characteristic fragmentation behavior of hydroquinone glycosides by electrospray ionization tandem mass spectrometry with optimization of collision energy. *Journal of mass spectrometry*. 2009;44(8):1182-1187.

78. Zhang Q, Xu J, Li X, Lian H, Chen H. Determination of morphine and codeine in urine using poly (dimethylsiloxane) microchip electrophoresis with electrochemical detection. *J Pharm Biomed Anal*. 2007;43(1):237-242.

79. Petersen NJ, Jensen H, Pedersen-Bjergaard S. On-chip electromembrane extraction for monitoring drug metabolism in real time by electrospray ionization mass spectrometry. *Microchip Capillary Electrophoresis Protocols*. 2015:171-182.

80. Qiang W, Zhai C, Lei J, et al. Disposable microfluidic device with ultraviolet detection for highly resolved screening of illicit drugs. *Analyst*. 2009;134(9):1834-1839.

81. Greenwood PA, Merrin C, McCreedy T, Greenway GM. Chemiluminescence µTAS for the determination of atropine and pethidine. *Talanta*. 2002;56(3):539-545.

82. Bell SC, Hanes RD. A microfluidic device for presumptive testing of controlled substances. *J Forensic Sci*. 2007;52(4):884-888.

83. Musile G, Wang L, Bottoms J, Tagliaro F, McCord B. The development of paper microfluidic devices for presumptive drug detection. *Analytical Methods*. 2015;7(19):8025-8033.

84. Sheng J, Ping Q, Lei J, Ju H, Song C, Zhang D. Fast and high-performance screening of narcotic drugs on a microfluidic device by micellar electrokinetic capillary chromatography. *Anal Lett*. 2012;45(7):652-664.

85. Greenway GM, Nelstrop LJ, Port SN. Tris (2, 2-bipyridyl) ruthenium (II) chemiluminescence in a microflow injection system for codeine determination. *Anal Chim Acta*. 2000;405(1-2):43-50.

86. Smith F. *Handbook of forensic drug analysis.* Elsevier; 2004.

87. Reyes-Garcés N, Bojko B, Pawliszyn J. High throughput quantification of prohibited substances in plasma using thin film solid phase microextraction. *Journal of Chromatography A*. 2014;1374:40-49.

88. Jain R, Singh R. Applications of dispersive liquid–liquid micro-extraction in forensic toxicology. *TrAC Trends in Analytical Chemistry*. 2016;75:227-237.

89. Kataoka H. Current developments and future trends in solid-phase microextraction techniques for pharmaceutical and biomedical analyses. *Analytical Sciences*. 2011;27(9):893.

90. Eckert WG. *Introduction to forensic sciences.* CRC press; 1996.

91. Ulrich S. Solid-phase microextraction in biomedical analysis. *Journal of Chromatography A*. 2000;902(1):167-194.

92. Yarin AL, Koombhongse S, Reneker DH. Bending instability in electrospinning of nanofibers. *J Appl Phys*. 2001;89(5):3018-3026.

93. Pan Q, Tong N, He N, et al. Electrospun mat of poly (vinyl alcohol)/graphene oxide for superior electrolyte performance. *ACS applied materials & interfaces*. 2018;10(9):7927-7934.

94. Yarin AL, Koombhongse S, Reneker DH. Taylor cone and jetting from liquid droplets in electrospinning of nanofibers. *J Appl Phys*. 2001;90(9):4836-4846.

95. Gao W, Havas D, Gupta S, et al. Is reduced graphene oxide favorable for nonprecious metal oxygen-reduction catalysts? *Carbon*. 2016;102:346-356.

96. Pan Q, Xie J, Liu S, Cao G, Zhu T, Zhao X. Facile one-pot synthesis of ultrathin NiS nanosheets anchored on graphene and the improved electrochemical li-storage properties. *Rsc Advances*. 2013;3(12):3899-3906.

97. Liu S, Xie J, Pan Q, et al. Graphene anchored with nanocrystal Fe2O3 with improved electrochemical li-storage properties. *Int.J.Electrochem.Sci*. 2012;7:354-362.

98. Wang R, Fu Y, Lai L. A new atom-additive method for calculating partition coefficients. *J Chem Inf Comput Sci*. 1997;37(3):615-621.

99. Tiwari A, Sekhar AK. Workflow based framework for life science informatics. *Computational biology and chemistry*. 2007;31(5-6):305-319.

100. Dhalla IA, Persaud N, Juurlink DN. Facing up to the prescription opioid crisis. *BMJ: British Medical Journal (Online)*. 2011;343.

101. Weiner SG, Malek SK, Price CN. The opioid crisis and its consequences. *Transplantation*. 2017;101(4):678-681.

102. Kolodny A, Courtwright DT, Hwang CS, et al. The prescription opioid and heroin crisis: A public health approach to an epidemic of addiction. *Annu Rev Public Health*. 2015;36:559-574.

103. FDA US. No title. *US Food and Drug Administration guidance for industry: bioanalytical method validation (2001)*.